⌘ *Author's Choice*

THE JOURNAL OF BIOLOGICAL CHEMISTRY VOL. 287, NO. 37, pp. 31280–31297, September 7, 2012

Multiple Novel Signals Mediate Thyroid Hormone Receptor Nuclear Import and Export*[S]

Received for publication, July 5, 2012 Published, JBC Papers in Press, July 19, 2012, DOI 10.1074/jbc.M112.397745

Manohara S. Mavinakere, Jeremy M. Powers[1], Kelly S. Subramanian, Vincent R. Roggero, and Lizabeth A. Allison[2]

From the Department of Biology, College of William and Mary, Williamsburg, Virginia 23187

Background: Thyroid hormone receptor (TR) shuttles between the cytosol and nucleus and regulates gene expression in response to hormone.
Results: TR shuttling is mediated by multiple, transferable nuclear localization and nuclear export signals.
Conclusion: Functional domains of TR work in concert to modulate shuttling.
Significance: Molecular characterization of signals that regulate shuttling is crucial for understanding nuclear receptor function.

Thyroid hormone receptor (TR) is a member of the nuclear receptor superfamily that shuttles between the cytosol and nucleus. The fine balance between nuclear import and export of TR has emerged as a critical control point for modulating thyroid hormone-responsive gene expression; however, sequence motifs of TR that mediate shuttling are not fully defined. Here, we characterized multiple signals that direct TR shuttling. Along with the known nuclear localization signal in the hinge domain, we identified a novel nuclear localization signal in the A/B domain of thyroid hormone receptor α1 that is absent in thyroid hormone receptor β1 and inactive in the oncoprotein v-ErbA. Our prior studies showed that thyroid hormone receptor α1 exits the nucleus through two pathways, one dependent on the export factor CRM1 and the other CRM1-independent. Here, we identified three novel CRM1-independent nuclear export signal (NES) motifs in the ligand-binding domain as follows: a highly conserved NES in helix 12 (NES-H12) and two additional NES sequences spanning helix 3 and helix 6, respectively. Mutations predicted to disrupt the α-helical structure resulted in a significant decrease in NES-H12 activity. The high degree of conservation of helix 12 suggests that this region may function as a key NES in other nuclear receptors. Furthermore, our mutagenesis studies on NES-H12 suggest that altered shuttling of thyroid hormone receptor β1 may be a contributing factor in resistance to thyroid hormone syndrome. Taken together, our findings provide a detailed mechanistic understanding of the multiple signals that work together to regulate TR shuttling and transcriptional activity, and they provide important insights into nuclear receptor function in general.

Protein transport into and out of the nucleus occurs through nuclear pore complexes embedded in the nuclear envelope. Import and export of proteins through the nuclear pore complexes are mediated by karyopherins, which bind to a nuclear localization signal (NLS)[3] or nuclear export signal (NES) present in the cargo protein. The most well studied NLS sequences are the classical monopartite and bipartite NLS motifs, exemplified by the simian virus 40 (SV40) large T-antigen NLS (PKKKRKV) and nucleoplasmin (KRPAATKKAGQAKKKK), respectively (1). Other nonclassical NLS motifs have been defined, and it is likely that many more remain uncharacterized. NES motifs have remained difficult to predict, with only the prototypical chromosome region maintenance 1 (CRM1)-dependent leucine-rich NES sequence being well characterized (2). In recent years the importance of regulated nucleocytoplasmic transport in gene regulation has become apparent, and there is strong interest in identifying novel NLS and NES motifs (3–5).

Our interest for many years has been in the mechanisms regulating the nuclear import and export of thyroid hormone receptor α1 (TRα1 and NR1A1a), a member of the nuclear receptor superfamily. Thyroid hormone receptors (TRs) are encoded by two genes, one for TRα and another for TRβ, which encode the major isoforms of TR, including TRα1, TRα2, TRβ1, and TRβ2. Both TRα1 and TRβ1 shuttle between the nucleus and cytoplasm; however, they localize primarily to the nucleus at steady state (6), where they either activate or repress target gene expression in response to thyroid hormone (7, 8). Nuclear localization is critical for the gene regulatory function of TR. For example, mislocalization of TRα1 to the cytoplasm by its oncogenic homolog v-ErbA may contribute to oncogenic conversion of cells (9, 10). It is clear that a comprehensive understanding of TR trafficking must take into account both nuclear import and export pathways.

Nuclear receptors share significant similarity in the DNA-binding domain (DBD), hinge region, and ligand-binding domain (LBD); however, they show variability in their N-termi-

* This work was supported, in whole or in part, by National Institutes of Health Grant R15 DK058028-03 from NIDDK (to L. A. A.). This work was also supported by National Science Foundation Grants MCB0646506 and MCB1120513 (to L. A. A.).
⌘ *Author's Choice*—Final version full access.
[S] This article contains supplemental Tables S1 and S2.
[1] Recipient of a scholarship from the ALSAM Foundation.
[2] To whom correspondence should be addressed: Dept. of Biology, College of William and Mary, 540 Landrum Dr., ISC 3035B, Williamsburg, VA. Tel.: 757-221-2232; Fax: 757-221-6483; E-mail: laalli@wm.edu.

[3] The abbreviations used are: NLS, nuclear localization signal; TR, thyroid hormone receptor; TRα1, thyroid hormone receptor α1; TRβ1, thyroid hormone receptor β1; NES, nuclear export signal; LMB, leptomycin B; T_3, thyroid hormone; DBD, DNA-binding domain; LBD, ligand-binding domain; GR, glucocorticoid receptor; AR, androgen receptor; G3, GFP-GST-GFP vector; CRM1, chromosome region maintenance 1; RTH, resistance to thyroid hormone; N, nuclear; C, cytosolic; TRE, thyroid hormone-responsive element.

nal A/B domain and in the region C-terminal to the LBD (11). Although an NLS in the hinge domain has been partially characterized for TRs (12–16), the corresponding complete NLS in the hinge domain of TRα1 had not been fully defined. However, a wealth of information regarding NLS motifs is available from other nuclear receptors. For example, the rat constitutive androstane receptor has a ligand-independent NLS in its hinge region, as well as a ligand-dependent NLS in its LBD (17, 18), whereas nuclear import of peroxisome proliferator-activated receptor α and γ is mediated by an NLS in the A/B domain and a second NLS that spans the DBD and hinge region (3). Highlighting the modular nature of nuclear receptors, the glucocorticoid receptor (GR) has a bipartite NLS in its DBD and a ligand-dependent NLS in its LBD (19–21), and the androgen receptor (AR) has a bipartite NLS in its DBD, a ligand-dependent NLS in its LBD, and putative NLS activity at its N terminus (22, 23). In contrast, only one NLS located in the DBD has been identified in the retinoid X receptor (24).

Many structural studies of TRα1 have been performed to correlate structural motifs with particular functions of the receptor. For example, the N-terminal A/B domain of nuclear receptors has a random coiled structure (25), and the LBD of TRα1 has 12 α-helices and four β-sheets (26). Helix 12, in addition to its role in ligand binding, also has a transactivation function termed AF-2 that is necessary for coactivator binding and release of corepressors upon ligand binding (27–29). Similarly, the A/B domain of TR has a transactivation function termed AF-1 (30–32). However, these previous studies did not address the question of whether known structural features of TRα1 include signals for nuclear import and export.

Our prior studies have revealed an increasingly complex picture of TRα1 nuclear export, involving multiple pathways and export factors. We have shown that TRα1 uses both the export factor CRM1 in cooperation with calreticulin for its nuclear export and a second CRM1-independent pathway (33). However, this study did not address the specific sequence determinants involved in nuclear export of TRα1. CRM1 mediates the nuclear export of proteins with leucine-rich NES sequences (34). Even though some members of the nuclear receptor family have CRM1-independent NES sequences, it is not known what other karyopherins are involved in these alternative export pathways (35). There is some limited information available on the protein cargos exported by these other karyopherins (36, 37); however, there is limited understanding of the sequence determinants for the export of proteins that use a CRM1-independent pathway.

In this report we have identified a novel NLS, designated NLS-2, in the A/B domain of TRα1 that is absent in TRβ1, and a novel, conserved CRM1-independent NES in the AF-2 region of helix 12 in the TRα1 LBD, designated NES-H12. Mutations in this NES markedly reduce both nuclear export and transactivation of thyroid hormone-mediated gene expression. We also provide evidence for additional NES activity in the region spanning helix 3 (NES-H3) and helix 6 (NES-H6) of the TRα1 LBD. The NLS and NES motifs were shown to be sufficient to target a cytosolic protein to the nucleus or a nuclear protein to the cytosol, respectively. In addition, NLS-2 and NES-H12 were shown to be necessary for efficient import or export in the context of the full-length receptor.

Conservation of targeting signals among the vertebrate species suggests that nucleocytoplasmic shuttling is crucial for the normal function of TRα1. Indeed, our mutagenesis studies point to the intriguing possibility that altered shuttling of TRβ1, due to defective nuclear export, may be a contributing factor in resistance to thyroid hormone syndrome. These findings highlight the complexity of the signals that regulate the shuttling of TR and emphasize the importance of detailed molecular characterization for understanding nuclear receptor function.

EXPERIMENTAL PROCEDURES

DNA Constructs—Rat TRα1 domains, NLS, and NES constructs, chicken TRα1 (cTRα1) A/B domain, and v-ErbA A/B domain (excluding the retroviral Gag sequence) were cloned as PCR products into a GFP-GST-GFP (G3) expression vector (designed by Ghislain Bonamy) as C-terminal tags. Oligonucleotides used for cloning were annealed, digested with the appropriate restriction endonuclease, and purified using a PCR purification kit (Qiagen, Valencia, CA). Digested oligonucleotides were ligated into the G3 vector. A/B domain mutations were made using QuikChange® mutagenesis kit according to the manufacturer's instructions (Agilent Technologies, Santa Clara, CA). Mutagenesis primers were designed using QuikChange® primer design program. GFP-TRα1 and GFP-v-ErbA expression vectors were constructed as described previously (6). The expression vector for GFP-tagged human TRβ1 (accession number BC106929), cloned into pReceiver-M29 vector, was obtained from Capital Biosciences (Rockville, MD). PCR primers and short oligonucleotides used in cloning were synthesized by Integrated DNA Technology (Coralville, IA). A list of primer pairs along with the cloning sites and the source vector used in this study are presented in supplemental Table S1. Sequences of individual primers and oligonucleotides are listed in supplemental Table S2.

Cell Culture and Transfection—HeLa cells (ATCC CCL-2) were cultured at 37 °C and 5% CO_2 in minimum Eagle's medium supplemented with 10% FBS, 100 units/ml penicillin, and 100 μg/ml streptomycin (Invitrogen). For transfection, $7.5–8.0 \times 10^5$ cells were plated on 40-mm coverslips (Bioptech, Butler, PA) in 60-mm plates. The next day cells were transfected with 1.5 μg of plasmid DNA using Lipofectamine 2000, according to the manufacturer's instructions (Invitrogen). Twenty four hours post-transfection, cells were analyzed by live cell imaging. For ligand-dependent nuclear translocation experiments, cells were cultured in medium supplemented with charcoal dextran-stripped FBS.

For FRAP analysis (see below), 4.5×10^5 HeLa cells were seeded in 35-mm glass bottom dishes (Mattek, Ashland, MA), followed by transfection with 0.75 μg of GFP-tagged TRα1 or TRβ1 expression plasmids and 1.5 μl of Lipofectamine 2000. In addition, cells were treated with 200 ng of cytochalasin D (Sigma) for 16 h (either pre-or post-transfection) to promote nuclear division in the absence of cytokinesis. Subsequently, cells were washed in minimum Eagle's medium to remove residual cytochalasin D for at least 23 h prior to FRAP analysis.

Live Cell Imaging—Cells were placed in a Focht Chamber System 2 (FCS2 ®, Bioptech) and maintained at 37 °C. MEM without supplements or phenol red was preincubated overnight at 37 °C and 5% CO_2, prior to use in live cell imaging experiments. Medium was replaced once per h for experiments lasting more than 1 h. Where indicated, medium contained 9.3 nM LMB (Sigma) and 100 nM T_3 (Sigma) to monitor CRM1-dependent nuclear export and ligand-dependent nuclear import. Images were captured using a Nikon Plan apo-60×/1.20 water immersion objective and a CoolSnap HQ2 CCD camera (Photometrics, Tucson, AZ). GFP was visualized using Blue Excitation, B-2E/C filter block (Nikon). Image capturing and analysis were carried out using Nikon NIS-elements Version 3.1. For time lapse imaging experiments, images were captured at 3-min intervals.

Cell Counts and Quantification of Nuclear Transport Activity—The intracellular distribution patterns of NES and NLS constructs were visualized by GFP fluorescence in live cells, as described above. NLS constructs were scored in replicate experiments as primarily nuclear (N), nuclear accumulation and a clearly visible cytosolic population (N > C), whole cell (N ≤ C), and primarily cytosolic (C). The efficiency of nuclear import was measured as an increase in the number of cells with a primarily nuclear distribution of the NLS construct. NES constructs were scored in the same categories, except cells scored as N > C and N ≤ C were combined into one category (C). The efficiency of nuclear export was measured as an increase in the number of cells with a cytosolic localization of the NES constructs. Mutations that inhibit nuclear export showed an increase in nuclear retention.

Fluorescence Recovery after Photobleaching (FRAP) Analysis—The kinetics of shuttling of NES-H12 mutants and wild-type TRα1 and TRβ1 were carried out using FRAP analysis. All FRAP experiments were performed in an Okolab incubation system (Okolab, Italy) for a Nikon Ti-E PFS-A1 confocal system at 37 °C under 5% CO_2 and 37% humidity. Imaging was carried out using an Apo LWD 40× WIS DIC N2 objective. One of the two nuclei in a single multinucleated cell was photobleached at 45% laser power for 17 s using the 488 nm line. Fluorescence recovery of the bleached nucleus was monitored every 2 min for 16 min and every 5 min for another 50 min. Protein synthesis was inhibited by 25 μg/ml cycloheximide during the imaging period. Cell plasma membranes were visualized with CellMask™ deep red plasma membrane stain as per the manufacturer's instruction (Invitrogen). This labeling was used to confirm the presence of more than one nucleus in a single cell. For quantitative analysis of digitized images, fluorescent intensity values were generated using NIS-Elements AR (Nikon). Data were expressed as percent intensity of recovery. For TRβ1, time 0 was set as 2 min, to minimize the contribution of the small cytosolic population (≤ 15%) toward recovery rates. The recovery rate of mutant *versus* wild-type proteins was plotted for GFP-TRα1 and GFP-TRβ1.

Chloramphenicol Acetyltransferase (CAT) Enzyme-linked Immunosorbent Assay (ELISA)—HeLa cells were plated at 6.0–7.0 × 10^5 cells in 100-mm dishes and transiently transfected for 6–7 h with 5 μg of tk-TREp-CAT reporter plasmid containing a synthetic palindromic thyroid hormone-responsive element (TRE), and 5 μg of GFP-TRα1, GFP-TRβ1, or GFP-TRα1 mutant expression plasmids (GFP-TRα1 F401A, GFP-TRα1 F401P, GFP-TRα1 R26H), or 5 μg of empty vector (pCAT®3-Basic Vector). Medium was replaced 12 h post-transfection with MEM containing 10% charcoal-dextran stripped FBS (Invitrogen) supplemented with or without 100 nM T_3 (Sigma). After 12 h, cells were lysed, cell extracts prepared, and extracts were used to determine CAT expression levels by ELISA according to the manufacturer's specifications (Roche Applied Science). Protein concentration was determined by Nano Drop (ND-1000 Spectrophotometer) and adjusted to the same amount of total protein (600 μg). For each assay, a standard curve utilizing four pure protein standards was prepared, to ensure that CAT concentrations of sample extracts fell within the linear range of the assay. Replicate samples were assayed in each microplate.

RESULTS

Characterization of the Bipartite NLS Sequence of the TRα1 Hinge Region—Prior studies suggest that the hinge region of both TRα1 and TRβ1 contains a classical NLS (13, 14, 16). Although partially characterized for TRβ1 (14, 16), the NLS in the hinge domain of TRα1 has not been fully defined. To begin to map the hinge NLS in rat TRα1, we cloned the hinge region into a G3 vector for expression as C-terminal fusion protein with the G3 tag (Fig. 1*A*). The G3-Hinge fusion protein has a number of important properties; it can be tracked in real time in transiently transfected cells; it is too large for diffusion through the nuclear pore complex, and it serves the purpose of demonstrating that a putative NLS is sufficient to target G3, a cytosolic protein, to the nucleus.

The expression vector for G3-Hinge was transfected into HeLa cells, and the fusion protein was analyzed for its ability to localize to the nucleus or cytosol, in comparison with GFP-tagged full-length TRα1 and G3 alone (Fig. 1*B*). GFP-TRα1 has a predominantly nuclear localization, although G3 is entirely cytosolic. As expected, the hinge domain was sufficient to localize G3 to the nucleus. Based on earlier predictions for the hinge region NLS of TRα1 (38), a minimal sequence was cloned into the G3 vector. This minimal sequence of the hinge region, designated NLS-1 (KRVAKRKLIEQNRERRRK), was sufficient to target the G3 fusion protein to the nucleus (Fig. 1*B*). This bipartite NLS is well conserved in both the oncoprotein v-ErbA and TRβ1 (Fig. 1*C*).

A/B Domain of TRα1, But Not of TRβ1, Contains a Novel, Conserved Monopartite NLS—Earlier studies had shown that the hinge region of TRα1 only partially targeted a cytosolic protein to the nucleus (14, 39), thus pointing to the possibility of a second NLS within TRα1. When we used the program PSORT II (40) to search for NLS motifs, a potential NLS was identified in the TRα1 A/B domain. To determine whether TRα1 does indeed have a second NLS apart from NLS1 in the hinge domain, a G3-tagged TRα1 A/B domain fusion protein was examined for its intracellular distribution (Fig. 2*A*). In support of our predictions, the A/B domain construct localized to the nucleus, indicating that the A/B domain has an NLS sufficient to direct G3, a cytosolic protein, to the nucleus (Fig. 2*B*).

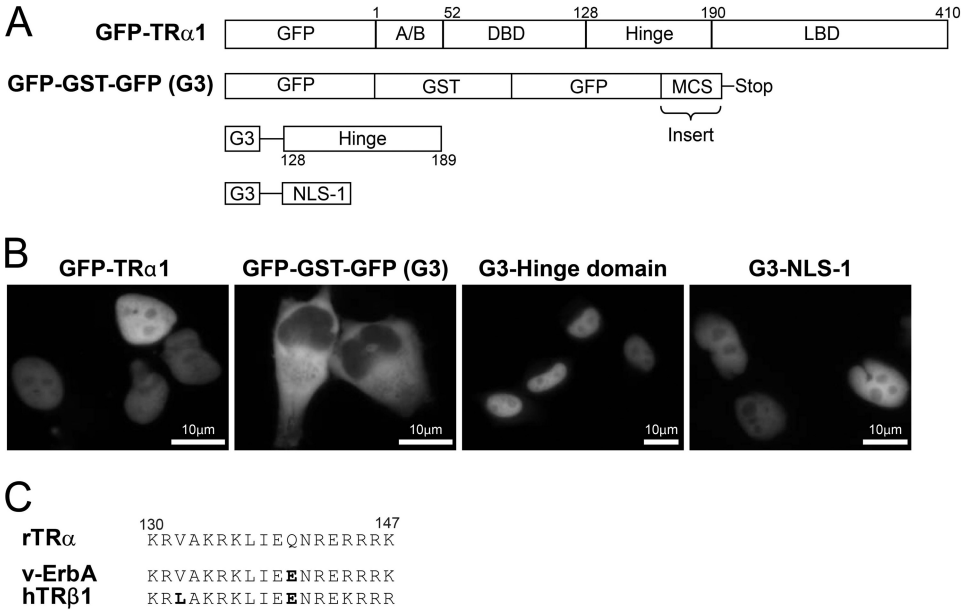

FIGURE 1. **TRα1 hinge region contains a bipartite NLS sequence, designated NLS-1.** *A,* schematic representation of full-length GFP-TRα1, G3 vector, and G3-tagged hinge domain and NLS-1 expression vectors (not drawn to scale). Abbreviations are as follows: *A/B*, A/B domain; *DBD*, DNA-binding domain; *Hinge*, hinge domain; *LBD*, ligand-binding domain; *MCS*; multiple cloning site. *B,* full-length TRα1, the hinge domain, and NLS-1 fusion proteins are predominantly nuclear, although the G3 vector is predominantly cytosolic. HeLa cells were transiently transfected with expression vectors, as indicated, 24 h prior to live cell imaging. *C,* alignment of NLS-1 shows that it is conserved among TRα1, TRβ1, and v-ErbA; amino acid changes are indicated in *bold*.

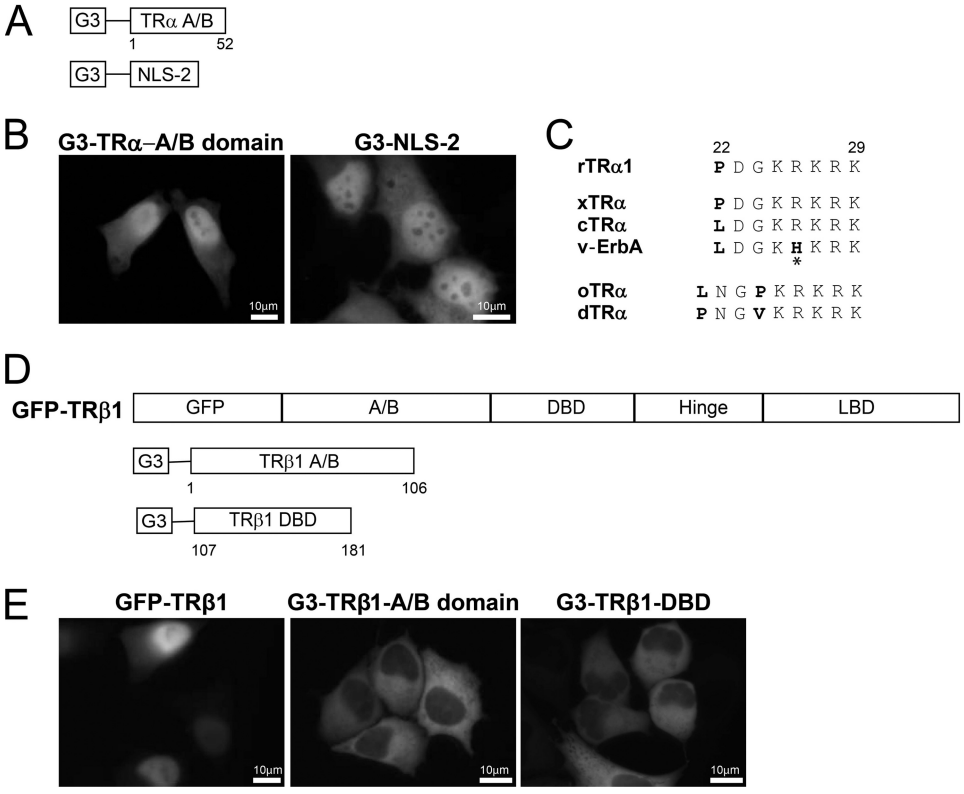

FIGURE 2. **TRα1 A/B domain contains a novel, conserved monopartite NLS, designated NLS-2.** *A,* schematic representation of G3-tagged A/B domain and NLS-2 expression vectors (not drawn to scale). *B,* A/B domain and NLS-2 fusion proteins localize to the nucleus. G3-tagged TRα1 A/B domain and NLS-2-expressing HeLa cells were imaged live as described in Fig. 1. *C,* alignment of rat (*r*) TRα1 NLS-2 with TRα from *Xenopus* (*x*), chicken (*c*), v-ErbA, *O. latipes* (*o*), and *D. rerio* (*d*) shows conservation across vertebrate species with some variation among fishes. Leucine and proline amino acid residues required for rat and chicken NLS-2 are in *bold* and also are shown in *bold* for dTRα and oTRα to indicate their likely participation in NLS function; the arginine to histidine change in v-ErbA is marked with an *asterisk*. *D,* schematic representation of full-length GFP-TRβ1 and G3-tagged TRβ1 A/B domain and DBD expression vectors (not drawn to the scale). *E,* TRβ1 A/B and DBD domain fusion proteins lack an NLS and remain cytosolic. GFP-TRβ1 and G3-tagged TRβ1 A/B domain and DBD-expressing HeLa cells were imaged as described in Fig. 1.

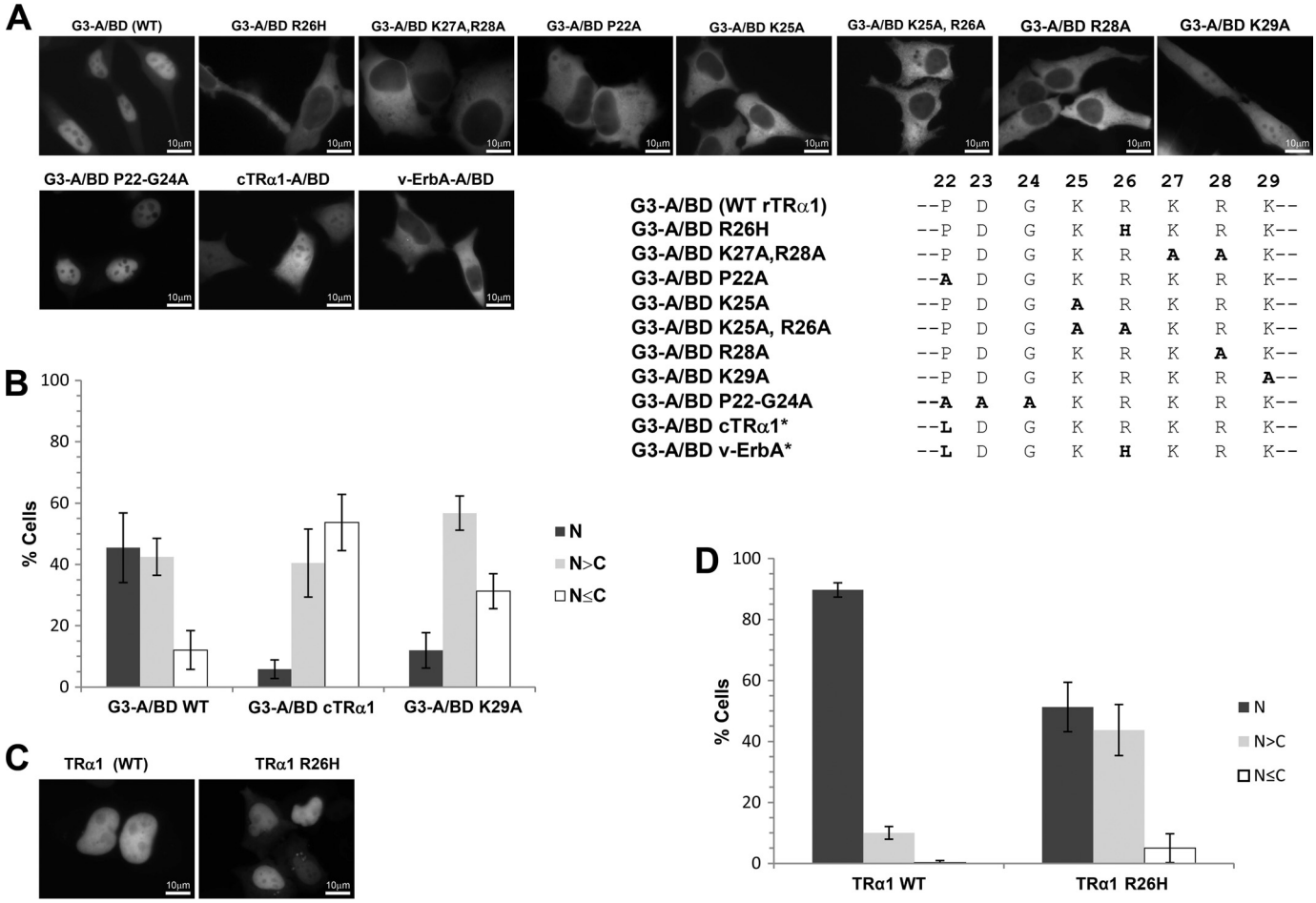

FIGURE 3. **Characterization of the essential amino acids residues required for nuclear translocation of the A/B domain and full-length TRα1.** *A,* A/B domain (A/BD) mutants of residues 22–29 show increased cytosolic distribution, except for A/BD P22-G34A, which remained primarily nuclear. Amino acid substitutions were introduced in the rTRα1 A/BD; changes are indicated in *bold* in the alignment of the A/BD mutants (residues 22–29). HeLa cells transfected with G3-tagged A/BD mutants were imaged as described in Fig. 1, and their distribution was compared with the rat TRα1 wild-type (*WT*) A/BD. *B,* chicken TRα1 (cTRα1) A/BD contains the weakest NLS activity. The *graph* summarizes the distribution of G3-tagged chicken TRα1 (cTRα1) A/BD, rTRα1 A/BD K29A, and WT A/BD constructs ($n = 7$, 115–150 cells were counted per replica). *Error bars* indicate ± S.D. *N*, primarily nuclear; $N > C$, nuclear accumulation with clearly visible cytosolic population; $N \leq C$, whole cell distribution pattern. *C,* arginine at position 26 is necessary for efficient nuclear localization of full-length TRα1. HeLa cells transfected with full-length GFP-rTRα1 (WT) or GFP-rTRα1 with the amino acid substitution R26H were imaged as described in Fig. 1. *D,* quantification of the distribution pattern of full-length TRα1 with the R26H mutation ($n = 5$; 109–142 cells counted per replica). *Error bars* indicate ± S.D.

To further characterize the novel NLS in the A/B domain of TRα1, we sought to determine the minimal sequence that confers NLS function. An NLS predicted by PSORT II is present within a single stretch of 8 amino acids, PDGKRKRK, suggesting that the NLS either has a pattern 7 motif, PDGKRKR, or pattern 4 motif, KRKR and RKRK. The nucleotide sequence encoding the complete 8-amino acid sequence was cloned into the G3 vector. This minimal sequence of the A/B domain, designated NLS-2, was sufficient to target the G3 fusion protein to the nucleus (Fig. 2*B*). Further analysis revealed that this sequence is well conserved among other vertebrate species (Fig. 2*C*), with some variations among chicken and fishes. Thus, NLS-2 includes a novel, monopartite NLS in the A/B domain of TRα1.

To determine whether TRβ1 has a second NLS apart from its previously characterized hinge domain NLS, G3-tagged TRβ1 A/B domain and DNA-binding domain (DBD) fusion proteins were examined for their intracellular distribution (Fig. 2, *D* and *E*). In striking contrast to TRα1, the A/B domain of TRβ1 was not sufficient to target G3 to the nucleus; the fusion protein remained cytosolic. Similarly, the DBD fusion protein also failed to translocate G3 into the nucleus. Based on these results we conclude that TRβ1 lacks a second NLS.

Identification of Essential Amino Acid Residues for NLS-2 Activity within A/B Domain—To define the essential amino acid residues for activity of TRα1 NLS-2, mutational studies were performed on the G3-tagged TRα1 A/B domain expression plasmid (see Fig. 2*A*). First, we investigated a naturally occurring A/B domain substitution in the oncoprotein v-ErbA, a highly mutated homolog of TRα1 that has a more cytosolic distribution than TRα1 (6). At the residue equivalent to arginine 26 in TRα1, v-ErbA has a histidine. Interestingly, a G3-TRα1 A/B domain fusion protein with the v-ErbA-equivalent substitution (G3-A/BD R26H) showed a cytosolic localization (Fig. 3*A*). Similarly, the A/B domain sequence of v-ErbA also showed a cytosolic distribution and failed to import G3 into the nucleus (Fig. 3*A*). Taken together, these results demonstrate that the R26H substitution abrogates the activity of NLS-2. Thus, this naturally occurring defect in NLS activity provides further insight into the molecular basis behind the oncogenic conversion of TRα1 into v-ErbA.

Next, to identify other critical amino acid residues for TRα1 NLS-2 function, alanines were substituted for the proline at residue 22 (P22A) and for each of the five basic residues from lysine 25 to Lys^{29}, either separately or in combinations (Fig. 3*A*). These alanine substitutions resulted in a dramatic change in the localization of the G3-A/BD fusion protein from primarily nuclear to completely cytosolic, except for G3-A/BD K29A, which showed a variable distribution. The change from lysine to alanine at position 29 resulted in a 33.6% decrease in the number of cells with a primarily nuclear distribution, compared with the wild-type A/B domain (G3-A/BD WT, Fig. 3*B*). Thus, the K29A mutation within the context of the A/B domain was compromised in NLS activity, whereas all other alanine mutations tested completely abolished NLS-2 activity.

The A/B domain NLS is well conserved in chicken TRα1 (cTRα1) except for a change from proline to leucine at the residue equivalent to Pro^{22} in rat TRα1. To determine whether the chicken A/B domain sequence has NLS activity despite this naturally occurring substitution, the entire cTRα1 A/B domain was cloned as a G3 fusion and tested for its localization. Only 5.8% of cells showed a primarily nuclear localization of the cTRα1 A/B domain, compared with 45.5% of cells showing a primarily nuclear localization of the rTRα1 A/B domain (Fig. 3*B*). Thus, the chicken TRα1 A/B domain has markedly reduced NLS activity in comparison with the rat TRα1 A/B domain.

To further examine the effect of the P22A mutation, alanine mutations were made that converted the three amino acids Pro^{22}–Asp^{23}–Gly^{24} to Ala residues (Pro^{22}-G24A). In striking contrast to the P22A mutant, the P22-G24A mutant predominantly localized to the nucleus, suggesting that the aspartic acid or glycine residue, or both together, interfere with the NLS activity of the A/B domain (Fig. 3*A*).

To confirm the importance of NLS-2 for efficient nuclear import in the context of the whole protein, we also introduced the R26H mutation into GFP-tagged full-length TRα1. This particular mutation was selected for analysis because R26H represents a physiologically relevant mutation in v-ErbA, the oncogenic homolog of TR (see Fig. 3*A*). Within the context of the whole protein, the R26H substitution resulted in a 38.4% decrease in the number of cells with a primarily nuclear localization, compared with wild-type TRα1 (Fig. 3, *C* and *D*). These results provide strong evidence that NLS-2 is necessary for directing efficient nuclear import of TR. When NLS-2 is defective, NLS-1 is unable to completely compensate, and overall nuclear accumulation is reduced.

Flanking Amino Acid Residues Have a Strong Negative or Positive Impact on NLS-2 Activity—To further confirm the minimal requirements for transferable NLS-2 function and to determine whether flanking amino acid residues influence NLS activity, a K29A mutant was constructed as an oligopeptide G3 fusion. The NLS-2-K29A oligopeptide showed a dramatic increase in the percentage of cells with a whole cell distribution (87.3% N $\leq$ C) (Fig. 4, *A* and *B*), in comparison with the K29A mutant in the A/B domain context (31.3% N $\leq$ C, see Fig. 3*B*). Thus, the strength of NLS-2 activity differs between the whole A/B domain context and the minimal oligopeptide context, suggesting that flanking amino acid residues are critical for the modulation of NLS activity.

To extend this analysis to other flanking sequences, we also tested an oligopeptide with the P22L substitution, to mimic the change from rat to chicken NLS-2. For cells expressing the G3-NLS-2-P22L fusion protein, 65.8% showed a whole cell distribution, compared with only 40.2% for cells expressing wild-type (WT) rat G3-NLS-2 (Fig. 4, *A* and *B*). Taken together, these results further confirm that the chicken NLS-2 has reduced nuclear targeting efficiency. Notably, when the P22L substitution is present in combination with v-ErbA R26H substitution, the G3-tagged oligopeptide (G3-NLS-2-P22L,R26H) remains entirely cytosolic (Fig. 4*A*).

Next, to determine more fully whether sequence context is of importance for NLS activity, we significantly altered the flanking sequences surrounding NLS-2. Strikingly, an oligopeptide fusion protein with the five basic amino acids of NLS-2 flanked by alanine residues (^{23}AAKRKRKA^{30}) still was able to function efficiently as an NLS (NLS-2–5K/R); the fusion protein was primarily localized to the nucleus (Fig. 4*A*). Thus, in this sequence context, the KRKRK sequence is sufficient for transferable NLS function.

Finally, mutagenesis was carried out to confirm the importance of the three amino acid residues N-terminal to the KRKRK sequence. Mutations were made in the context of a flanking alanine residue at position 22; this altered NLS-2 was designated NLS-2* and was subject to additional mutagenesis. NLS-2*-P22A and NLS-2*-P22A,G24A had a comparable distribution with only 16.3 and 7.8% of cells, respectively, showing a nuclear distribution of the G3 fusion proteins (Fig. 4, *C* and *D*). However, NLS2*-P22A,D23A resulted in a dramatic reversal of the distribution pattern; 77.9% of cells showed a predominantly nuclear localization of the G3 fusion protein. Thus, these results clearly demonstrate that Asp^{23} is the key amino acid residue that reduces the relative strength of wild-type NLS-2 activity. The extent of this influence varies based on the flanking sequence context.

Taken together, our data show that the presence of aspartic acid interferes with NLS-2 function. The presence of Pro or Leu at residue 22, however, counters the inhibitory influence of intervening nonbasic amino acids in the whole A/B domain context in both rat TRα1 and chicken TRα1 (see Fig. 3*B*). However, Pro, Leu, and Asp residues have less of an impact on NLS activity in the context of oligopeptide fusions (Fig. 4). These findings highlight the challenge of defining the minimal amino acid sequence for NLS activity; sequence context is of critical importance; flanking amino acids may have a strong negative or positive impact on NLS function.

Interplay between Domains Mediating TRα1 Subcellular Distribution—To investigate the interplay between different domains in mediating shuttling of TRα1, several combinations of individual domains were analyzed for their nucleocytoplasmic distribution (Fig. 5*A*). In contrast to the A/B and hinge domains that harbor NLS-2 and NLS-1 (see Figs. 1 and 2), respectively, G3-DBD and G3-LBD fusion proteins remained cytosolic (Fig. 5*A*).

Previously, it was reported that the DBD of TRβ is sufficient to confer nuclear export when fused to GFP; the DBD is

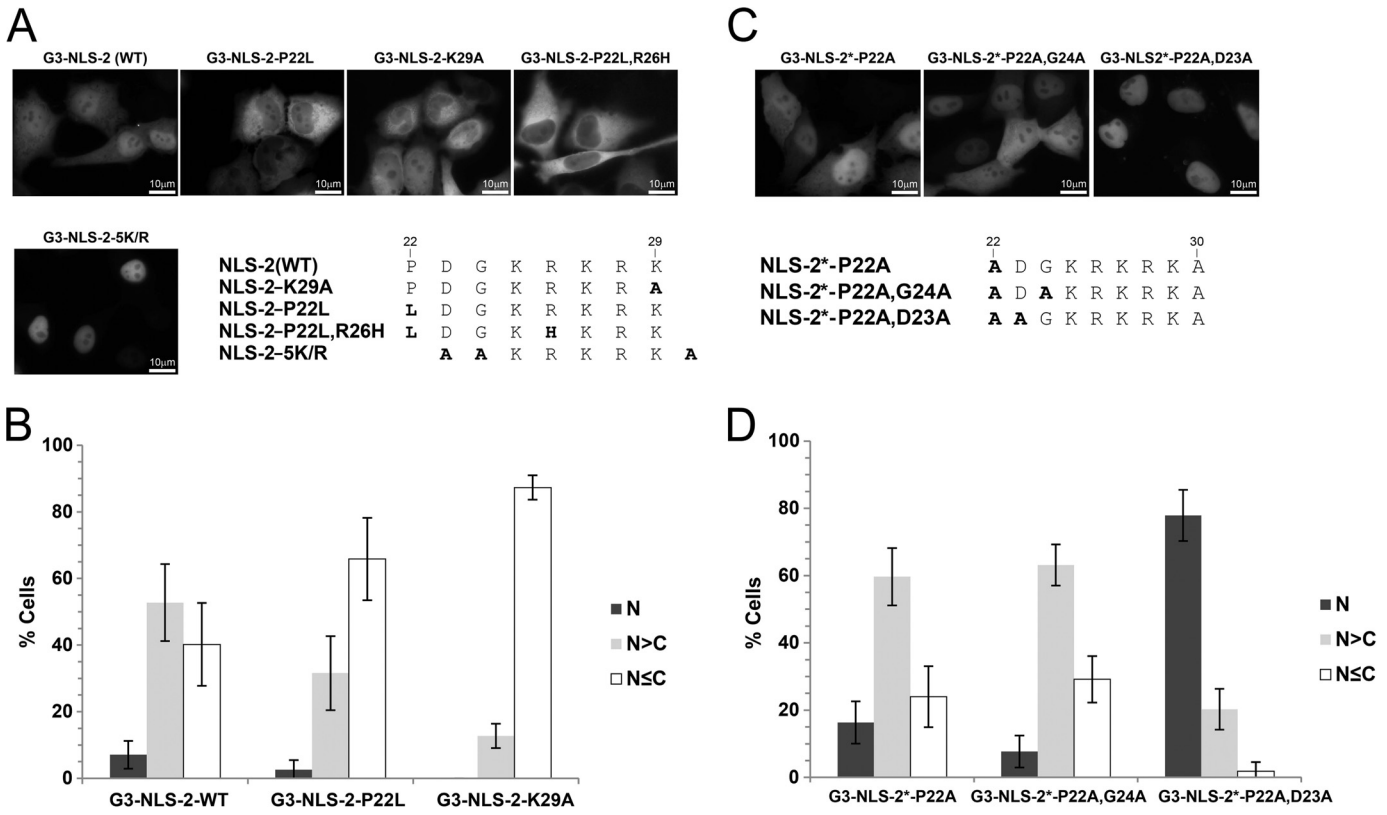

FIGURE 4. **Characterization of the minimal essential amino acid residues required for transferable NLS-2 activity.** *A,* amino acid substitutions were introduced in NLS-2 (oligopeptide mutants), as indicated in *bold*. HeLa cells transfected with G3-tagged NLS-2 mutants were imaged as described in Fig. 1, and their distribution was compared with the wild-type (*WT*) NLS-2. *B,* quantification of the distribution patterns of NLS-2-P22L and NLS-2 K29A ($n = 5–7$; 120–156 cells counted per replica). *Error bars* indicate ± S.D. *N*, primarily nuclear; $N > C$, nuclear accumulation with clearly visible cytosolic population; $N \leq C$, whole cell distribution pattern. *C,* aspartic acid residue at position 23 abrogates NLS-2 activity. G3-tagged NLS-2 mutants with a flanking alanine residue at position 22, designated NLS-2*, were constructed as indicated and analyzed for their subcellular localization in live cells. *D,* quantification of NLS-2* mutant distribution patterns. NLS-2*-P22A and NLS-2*-P22AG24A showed an increase in the population of cells with a cytosolic distribution of the mutants, whereas NLS-2*-P22AD23A showed a predominantly nuclear localization with minimal cytosolic distribution. ($n = 7$, 118–157 cells counted per replica). *Error bars* indicate ± S.D.

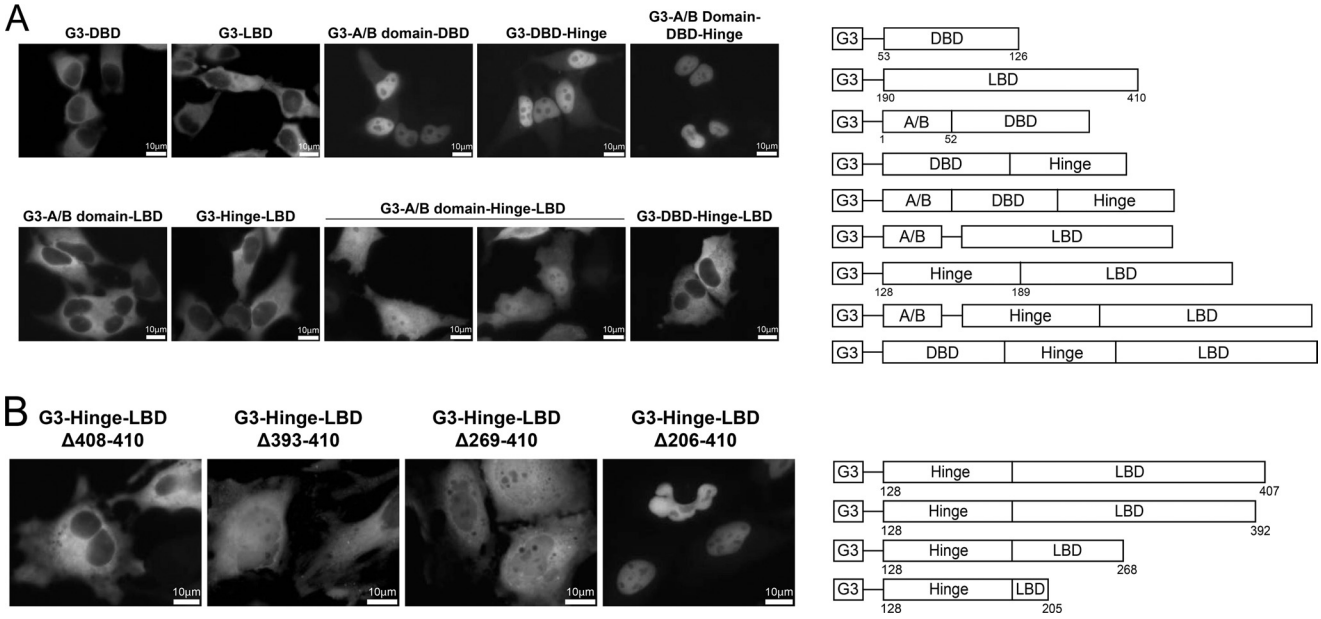

FIGURE 5. **Interplay between domains mediating TRα1 subcellular distribution.** *A,* LBD contains strong NES activity. *Left panels,* G3-tagged TRα1 domain expression constructs were transfected in HeLa cells and imaged as described in Fig. 1. *Right panel,* schematic representations of G3-tagged combinations of the A/B domain, hinge domain, DBD, and LBD expression constructs (not drawn to scale). Abbreviations are as described in Fig. 1. *B,* one or more NES motifs are present in the region from residues 206 to 265. *Left panels,* G3-tagged TRα1 domain expression constructs were transfected in HeLa cells and imaged as described in Fig. 1. *Right panel,* schematic representations of G3-tagged Hinge-LBD deletion constructs (not drawn to scale).

thought to be a binding site for calreticulin (41). Because we have shown that calreticulin also plays a role in TRα1 nuclear export (33), we sought to determine whether the TRα1 DBD would be sufficient to shift the balance of the A/B domain construct, containing NLS-2, from the nucleus to the cytosol. However, there was no appreciable change in the extent of nuclear localization of the G3-A/B domain-DBD fusion protein in comparison with the A/B domain alone (compare Fig. 5*A* with Fig. 2*A*). Similarly, DBD-Hinge domain and A/B domain-DBD-Hinge domain fusion proteins were also localized to the nucleus; their distributions were comparable with the hinge domain-only construct that contains NLS-1 (compare Figs. 5*A* with 1*B*). Taken together, these findings suggest that either the DBD lacks NES activity or that it has only a very weak NES that is dominated by both NLS-1 and NLS-2.

In striking contrast, G3-A/B domain-LBD and G3-Hinge-LBD fusion proteins were entirely localized to the cytosol (Fig. 5*A*), suggesting that the LBD has strong NES function. Next, a construct composed of the A/B domain, hinge domain, and LBD was tested for its ability to localize to the nucleus. This construct, despite including both NLS-1 and NLS-2, still showed a variable distribution ranging from nuclear in some cells to a whole cell distribution in others (Fig. 5*A*). Another contributing factor to this dramatic shift in localization from nuclear to cytosolic could be a concomitant decrease in nuclear retention, given that the DBD was not included in this construct. Previously, we showed that mutations that disrupt DNA binding result in decreased nuclear retention and increased cytosolic localization of TRβ1 (6). Therefore, to determine whether nuclear retention by the DBD counters NES activity in the LBD, a DBD-Hinge-LBD construct was tested for its ability to localize to the nucleus. Interestingly, this combination also showed a primarily cytosolic localization (Fig. 5*A*), suggesting that addition of the DBD is not sufficient for the nuclear retention of the Hinge-LBD construct. Taken together, our findings suggest that a more complete domain structure is important for the efficient nuclear localization of TRα1, in combination with the targeting signals present in NLS-1 and NLS-2.

TRα1 LBD Harbors Multiple NES Motifs—To identify the NES sequence(s) in the LBD, we tested progressive deletions of the LBD for loss of NES activity (Fig. 5*B*). Deletion mutants were constructed as G3-Hinge-LBD fusion proteins. As shown in Fig. 5*B*, the G3-Hinge-LBD fusion protein is localized to the cytosol. Because the hinge domain contains NLS-1, we reasoned that deleting an NES would lead to nuclear localization of Hinge-LBD deletion mutants. When three amino acids were deleted from the C terminus (Hinge-LBD Δ408–410), the mutant remained entirely cytosolic (Fig. 5*B*). However, progressive deletion of additional amino acids from the C terminus resulted in a concomitant increase in nuclear localization. When most of the LBD was deleted (Hinge-LBD Δ206–410), nuclear localization of the fusion protein was mediated by NLS-1 in the hinge domain. Deletion of amino acids 206–268, which includes helices 3–6, and deletion of the amino acids 393–407, which includes helix 12, showed significant nuclear accumulation. These results further suggest that one or more NES motifs are present in the region from residues 206 to 268 and 393 to 407 of the LBD.

Identification of Essential Amino Acid Residues for NES Activity in Three Conserved Helical Regions of the LBD—To further define the regions with NES activity in TRα1, we focused on the highly conserved helical regions within the LBD. First, we tested helix 12 (H12) for transferable NES activity. The region from residues 390 to 407 of the TRα1 LBD was able to partially export G3-Hinge, a nucleus-localized protein, to the cytosol, indicating that residues 390–407 harbor transferable NES activity, designated NES-H12 (Fig. 6*A*). We hypothesized that by adding one more copy of NES-H12, the export activity of the combined NES copies would shift the distribution of the G3-Hinge fusion protein even more toward the cytosol. Compared with the single copy NES-H12 construct, the NES-H12 double copy construct showed an increase in the number of cells with a distribution pattern ranging from whole cell to predominantly cytosolic (Fig. 6*A*). Thus, this result further confirmed that NES-H12 is a transferable NES.

To determine whether the region spanning helices H3 to H6 of TRα1 (residues 209–265) has a transferable NES, we analyzed the distribution of a G3-NES-H3/H6-Hinge fusion protein. The presence of the NES-H3/H6 region was sufficient to shift the distribution of the G3-Hinge nuclear protein toward the cytosol (compare Fig. 6, *A* with *B*); the G3-NES-H3/H6-Hinge fusion protein showed a distribution ranging from whole cell to predominantly cytosolic. These data suggest that one or more NES motifs reside in the H3/H6 region. This region is well conserved in TRβ1 and v-ErbA; thus, we predict that the H3/H6 region in these variants also has NES function.

The H3/H6 region is 57 amino acids long. As classical NES motifs, including NES-H12, are short peptides of less than 20 amino acids in length, we sought to identify the minimal sequence of H3/H6 that is required for nuclear export. Based on secondary structure predictions, the H3/H6 region was cloned as two fragments; one fragment included the helix 3 region, and the second fragment included the helix 6 region. Both fragments were cloned N-terminal to the hinge domain, similar to the NES-H12 construct. Surprisingly, G3-NES-H3-Hinge and G3-NES-H6-Hinge fusion proteins both showed an increased cytosolic distribution, in comparison with the G3-Hinge fusion protein alone (compare Fig. 6, *C* and *D* with *A*).

To further explore the NES activities of the H3 and H6 regions, we next cloned each of these sequences adjacent to NES-H12 toward the C-terminal end. The resulting G3-tagged NES-H3+H12-Hinge and NES-H6+H12-Hinge constructs showed marked increases in cytosolic distribution, compared with H3 or H6 alone, ranging from whole cell to cytosolic (Fig. 6, *C* and *D*). Based on these results, we concluded that the H3 and H6 regions have separate NES function and, hence, we designated these as NES-H3 and NES-H6, respectively. NES-H3 is well conserved among TR variants with a single amino acid change in v-ErbA and hTRβ1, respectively. Similarly, NES-H6 is fully conserved among TR variants, except for TRβ1, which has one amino acid change (Fig. 6, *C* and *D*).

It is important to point out that, as defined here, NES-H3 and NES-H6 share a proline and a methionine in common; present at the C terminus in NES-H3 and at the N terminus of NES-H6 (see Fig. 6, *C* and *D*). Attempts to clone shorter nonoverlapping fragments in different combinations did not yield any signifi-

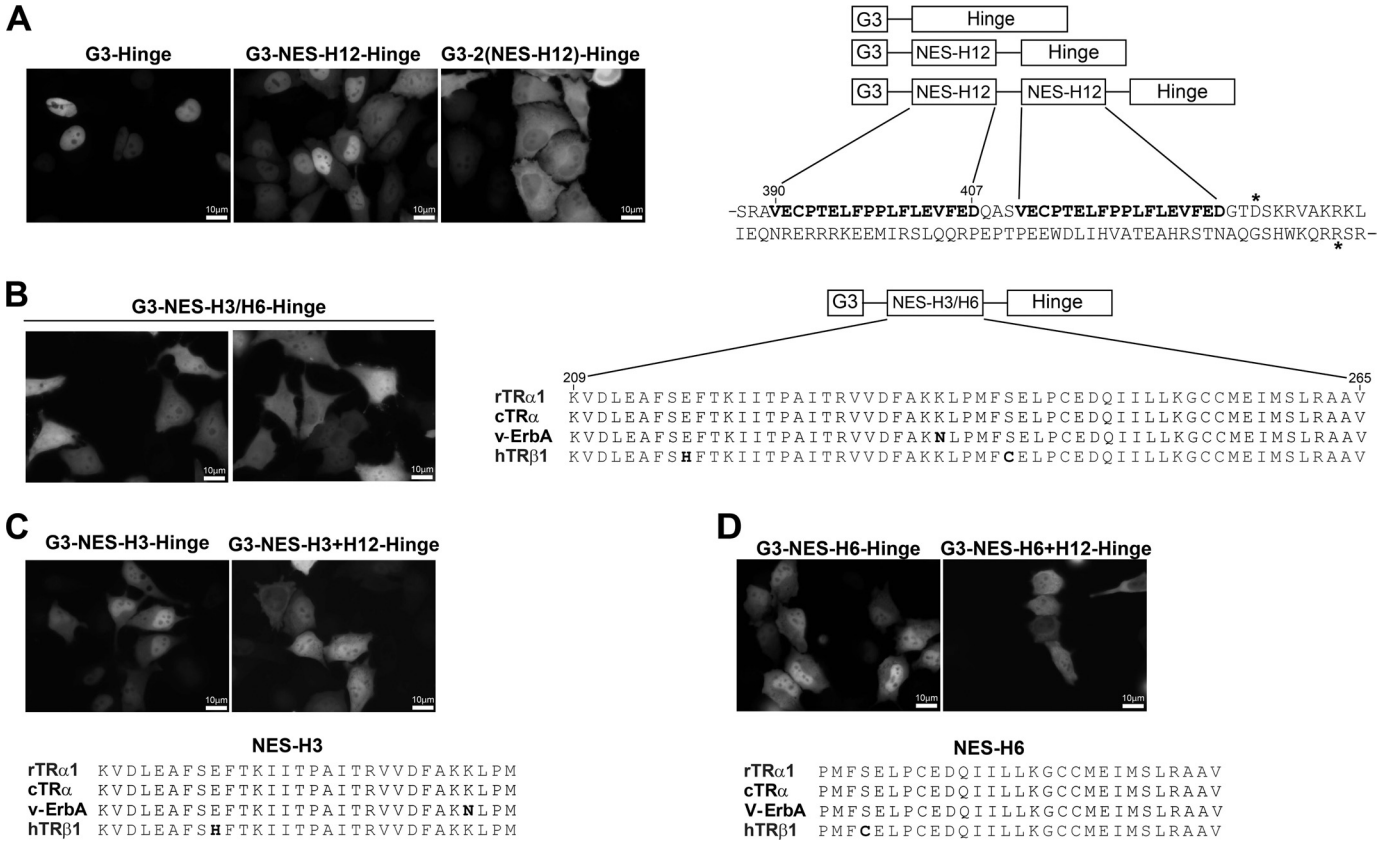

FIGURE 6. **TRα1 LBD has three independent transferable NES sequences.** *A,* NES-H12 is a transferable NES, and multiple NES motifs have an additive effect on nuclear export. *Left panels,* HeLa cells were transfected with G3-tagged TRα1 hinge domain constructs with either a single or double copy of NES-H12, as indicated. *Right panel,* schematic representations of the single or double copy minimal NES sequence in helix H12 (NES-H12, residues 390–407). The sequence of the NES-H12 double copy construct is shown with the NES in *bold*; the *asterisk* indicates the beginning and end of the hinge domain sequence. *B,* H3-H6 helix region harbors NES activity. *Left panels,* HeLa cells were transfected with G3-tagged TRα1 hinge domain constructs with NES-H3/H6 (residues 209–265), and live cells were imaged. *Right panel,* schematic representation of the NES-H3/H6 construct, and alignment showing sequence conservation in chicken (*c*) TRα, v-ErbA and human (*h*) TRβ1. Amino acid residues that differ from rat (*r*) TRα1 NES-H3/H6 among other TR variants are in *bold*. *C,* NES-H3 is a transferable NES, and multiple NES motifs have an additive effect on nuclear export. HeLa cells were transfected with G3-tagged TRα1 hinge domain constructs with either NES-H3 or a second copy N-terminal to NES-H12. Alignment of NES-H3 along with corresponding TR variants with amino acid variants indicated in *bold* is shown. *D,* NES-H6 is a transferable NES, and multiple NES motifs have an additive effect on nuclear export. HeLa cells were transfected with G3-tagged TRα1 hinge domain constructs with either NES-H6 or a second copy N-terminal to NES-H12. Alignment of NES-H6 along with corresponding TR variants with amino acid variants indicated in *bold* is shown.

cant export function, suggesting that retaining the original secondary structure is critical for NES activity. Thus, based on secondary structure prediction, the Pro and Met residues were retained in both sequences to keep this proposed structure intact. Given our experimental results and structural predictions, we currently classify NES-H3 and NES-H6 as independent NES motifs, rather than a single bipartite NES, although further analysis will be required to confirm this model unequivocally.

Dominant NES Activity in the LBD of TRα1 is CRM1-independent—LMB is a specific inhibitor of CRM1-dependent nuclear export. To determine whether the dominant NES activity in the LBD of TRα1 is CRM1-dependent or -independent, live cell imaging on cells transfected with various mutant constructs was carried out in the presence of LMB (Fig. 7). The oncoprotein v-ErbA, shown here for comparison, shuttles rapidly between the cytoplasm and nucleus; export is mediated by a strong CRM1-dependent NES in the N-terminal Gag region (42). As expected, the subcellular distribution of GFP-tagged v-ErbA shifted from predominantly cytosolic to predominantly nuclear after 60–90 min of LMB treatment, because CRM1-dependent export was inhibited.

Other nuclear receptors, such as GR and AR, contain ligand-dependent NLS sequences in the LBD; thus, we first sought to ascertain whether the LBD of TRα1 harbors a ligand-dependent NLS that might add to the complexity of analysis. HeLa cells transfected with G3-LBD expression vectors were treated with thyroid hormone (T_3) and LMB. Upon treatment, G3-LBD remained cytosolic (Fig. 7), suggesting that TRα1 does not have a ligand-dependent NLS in the LBD. However, this finding does not rule out the possibility that the LBD may contain a weak NLS that is dominated by strong CRM1-independent NES sequences in the LBD. In any event, the remainder of experiments was carried out in the absence of T_3, and the hinge region containing NLS-1 was included in constructs to provide nuclear import capability.

In contrast to v-ErbA, LMB treatment had no effect on the distribution of Hinge-LBD, DBD-Hinge-LBD, and Hinge-LBD Δ269–410 (which retains both NESH3 and NESH6); despite having NLS-1 in the hinge region, these fusion proteins

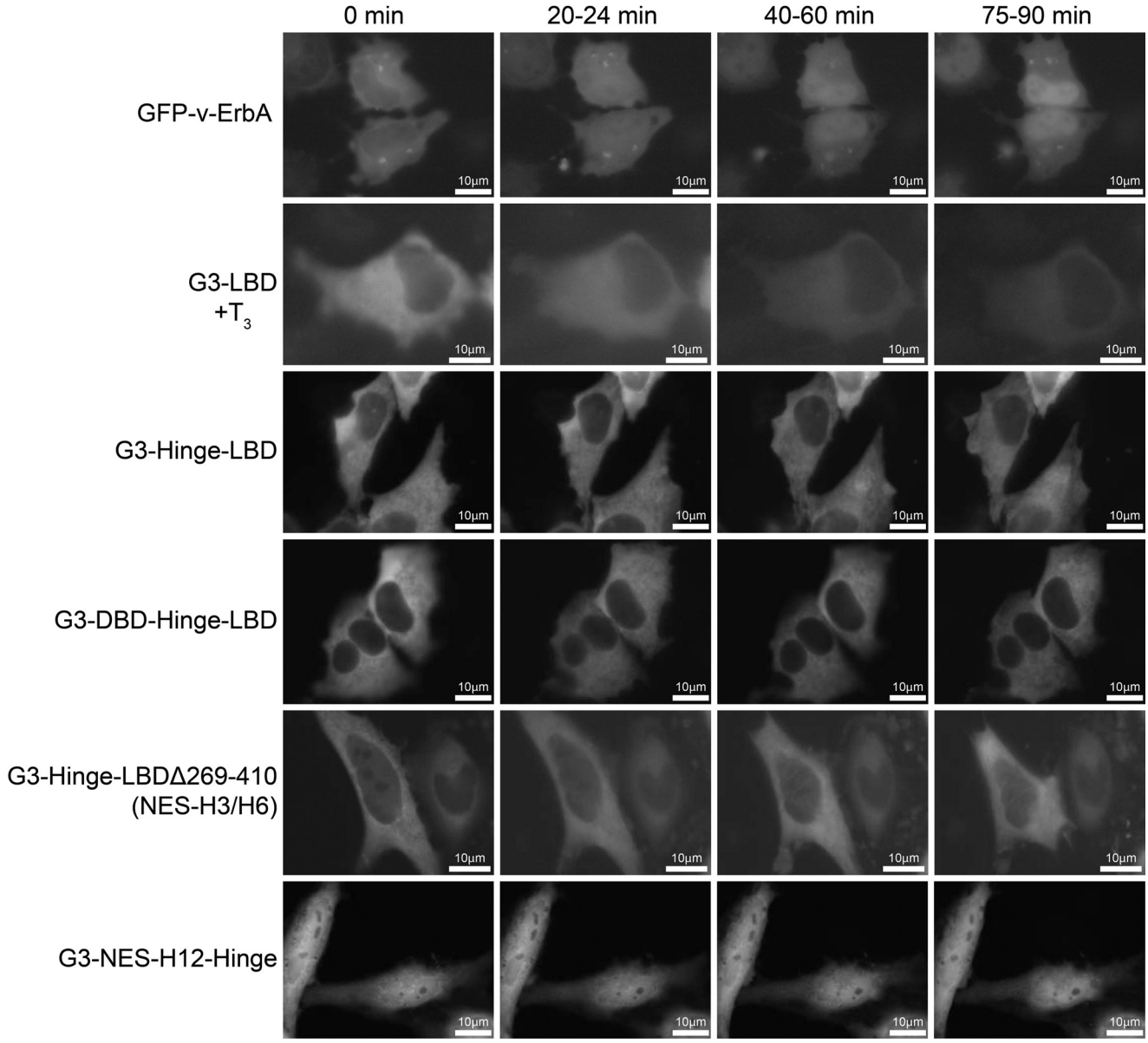

FIGURE 7. **Dominant NES activity in the TRα1 LBD is CRM1-independent.** v-ErbA and TRα1 domain constructs, as indicated, were transfected into HeLa cells, and sensitivity of export activity to leptomycin B was investigated by live cell imaging over a time course from 0 to 90 min. v-ErbA has a dominant CRM1-dependent NES and relocated from cytosol to nucleus within 60 min of treatment. The G3-tagged LBD (tested in the presence of T_3, to determine whether a ligand-inducible NLS was present), Hinge-LBD, DBD-Hinge-LBD, and Hinge-LBD Δ269–410 (contains NES-H3/H6 region) all remained cytosolic, and G3-NES-H12-Hinge remained whole cell, indicating that the NES functions in the LBD are CRM1-independent.

remained mostly cytosolic with no detectable accumulation in the nucleus over the time course (Fig. 7). Similarly, NES-H12-Hinge remained whole cell with no appreciable increase in nuclear accumulation, when cells were treated with LMB. Taken together, these results suggest that the dominant NES function in the LBD of TRα1 is CRM1-independent.

Characterization of Critical Amino Acids for NES-H12 Function—To determine the critical amino acids that are involved in NES-H12 functional activity, mutagenesis studies were performed on a hydrophobic residue-rich region within helix 12 (residues 390–407) (Fig. 8*A*). The cellular distribution of G3-tagged NES mutants was visualized in transfected cells. Data from replicate experiments are summarized in Fig. 8*B*.

A single amino acid change of phenylalanine to alanine at residue 401 (F401A) resulted in a 12% decrease in the number of cells with a cytosolic distribution in comparison with the wild-type NES. A mutant NES with two amino acid residue changes, F397A and F401A, showed a 19.5% decrease in the number of cells with a cytosolic distribution in comparison with wild type. When four hydrophobic amino acid residues (L400A, F401A, V404A, and F405A) were replaced by alanine in the L4(A) mutant, there was a 24% decrease in the number of cells with a cytosolic distribution relative to the wild-type NES-H12 (Fig. 8*B*). Thus, replacement of multiple hydrophobic residues with alanine had a major inhibitory effect on NES-H12 export activity, whereas alanine replacement of individual hydrophobic residues had only modest effects on the efficiency of NES-H12. Taken together, results suggest that multiple hydrophobic amino acids are required for efficient NES-H12 export activity.

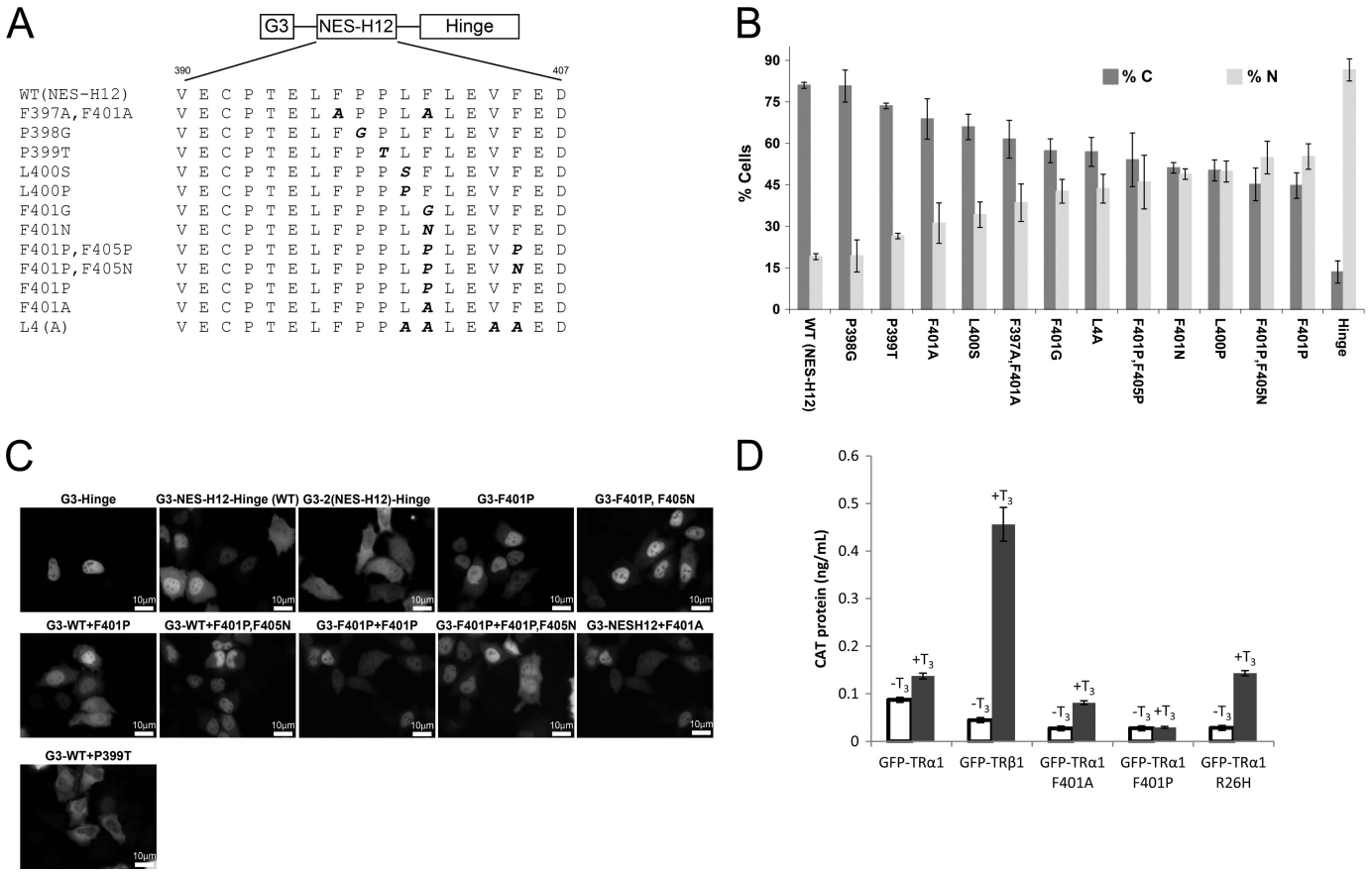

FIGURE 8. **Multiple hydrophobic residues contribute to NES-H12 activity.** *A,* amino acid changes made in NES-H12 are shown in *bold italics*. The mutant construct name and the corresponding amino acid substitutions are as indicated, except for L4(A) which represents a L400A, F401A, V404A, and F405A construct. *B,* nuclear export of individual mutations was quantified as a measure of the percentage of cells showing a clearly visible cytosolic or whole cell population (denoted as *C*) or a nuclear distribution (*N*). Mutant constructs are arranged in order of decreasing nuclear export activity. The hinge domain construct was used as a control for nucleus-only distribution. Data presented are averaged from three independent experiments for the mutant NES constructs and five independent experiments each for NES-H12-WT and hinge domain-only constructs. The average number of cells counted was 530 per replicate (ranging from 369 to 873 per sample). *Error bars* indicate ± S.D. *C,* double copy NES-H12 mutants show a significant reduction in NES activity. HeLa cells were transfected with expression constructs for G3-tagged NES-H12 mutants, with mutations in one or both copies of NES-H12 as indicated, and analyzed by live cell imaging. *D,* mutations in NES-H12 decrease T_3-mediated gene expression. HeLa cells were transiently transfected with 5 μg of tk-TREp-CAT reporter plasmid and 5 μg of full-length GFP-tagged TRα1, TRβ1, or TRα1 mutant expression plasmids (NES-H12 mutants F401A and F401P, and NLS-2 mutant R26H) in the presence of 100 nM T_3 (*black bar*) or in the absence of T_3 (*white bar*). CAT protein expression was quantified (ng/ml) based on measurements of CAT protein levels by ELISA. No basal levels of CAT protein were measured in HeLa cells transfected with 5 μg of empty vector and 5 μg of GFP-TRα1 with or without T_3 (data not shown). *Error bars* indicate ± S.D. ($n = 4$).

Our secondary structure predictions using the programs HNN and PSIPRED (43, 44) suggested that alanine replacement of hydrophobic residues may not completely disrupt the α-helical structure of H12, particularly for mutants F401A and F397A,F401A. Therefore, amino acids predicted to make significant changes to the NES-H12 secondary structure were selected for the next set of mutations. The phenylalanine at residue 401 in the core hydrophobic region of NES-H12 was replaced by glycine (F401G), proline (F401P), or asparagine (F401N). These changes resulted in a reduction in the number of cells with a cytosolic distribution of the fusion proteins for all the three mutations as follows: F401G showed a 23% reduction; F401P a 36% reduction, and F401N a 30% reduction in comparison with the wild-type NES-H12 (Fig. 8*B*). Likewise, substitution of a proline for a leucine at residue 400 (L400P) that was predicted to disrupt the α-helical structure of NESH12 resulted in a 31% decrease in the number of cells with a cytosolic distribution, similar to the F401P and F401N single amino acid changes (Fig. 8*B*).

To further investigate the effects of disrupting the secondary structure of NES-H12, double mutants were constructed with amino acid substitutions at residues 401 and 405. We predicted that these mutants would completely disrupt the α-helical structure of NES-H12, and thus, we hypothesized that these mutants would show complete inactivation of nuclear export. However, F401P,F405P and F401P,F405N showed only 27 and 36% decreases, respectively, in the number of cells with a cytosolic distribution in comparison with wild-type (WT) NES-H12 (Fig. 8*B*). These findings suggest that the NES-H12 mutants retain an active structural arrangement that is not adequately predicted by the programs HNN and PSIPRED.

Based on these results, it was predicted that replacing one of the prolines in H12 with a different type of helix-breaking amino acid would have minimal or no effect on NES-H12 activity. To test this prediction, a proline to glycine (P398G) change was introduced. As expected, this change did not result in a decrease in the nuclear export of the fusion protein in comparison with wild-type (WT) NES-H12 (Fig. 8*B*). However, as

noted above substituting a hydrophobic residue with a helix-breaking residue at position 401 (F401G) resulted in a significant decrease in nuclear export.

The H12 region is fully conserved between TRα1 and TRβ1, except for the presence of three additional amino acids toward the C terminus in TRα1. A number of mutations have been identified in the H12 region of TRβ1 in patients with resistance to thyroid hormone (RTH) syndrome (45). Some of the characteristics observed among the TRβ1 mutants include reduced ligand binding and increased corepressor binding that result in constitutive repression of T_3-responsive target genes. In some cases, the underlying molecular mechanism for disease pathology is unknown. Given that these mutations are within NES-H12, we sought to determine whether some of these mutations also affect nuclear export activity.

Two such TRβ1 RTH mutants were tested in this study. For ease of comparison with other H12 mutants in Fig. 8, we have maintained the residue numbering used for TRα1. Mutant L400S (equivalent to TRβ1 L454S) showed a 15% decrease in the number of cells with a cytosolic distribution in comparison with wild type, although mutant P399T (equivalent to TRβ1 P453T) only showed a 7.5% decrease in the number of cells with a cytosolic distribution (Fig. 8*B*). These data suggest that alteration of the conserved hydrophobic residues in the NES, in particular L454S in TRβ1, may result in increased nuclear retention of the receptor and reduced export activity, thereby interfering with the normal function of TRβ1.

To further confirm the critical role of the phenylalanine residues at positions 401 and 405 for NES-H12 function, we tested an additional panel of NES-H12 mutants. Because we showed that a double copy of NES-H12 in the G3-2(NES-H12)-Hinge construct had increased nuclear export activity (see Fig. 6*A*), we hypothesized that introduction of mutations in one or both copies of NES-H12 would result in a change in distribution from predominantly cytosolic to predominantly nuclear.

NES-H12+F401A showed an enhanced nuclear distribution in comparison with the NES-H12 double copy construct (Fig. 8*C*). Conversely, NES-H12 WT+P399T showed a cytosolic distribution similar to the NES-H12 double copy. These experiments further demonstrate that the F401A mutation significantly inhibits nuclear export function of NES-H12, whereas P399T only has a minimal effect.

Additional mutagenesis revealed that NES-H12 (WT)+F401P and WT+F401P,F405N remained predominantly nuclear, in comparison with the construct with a double copy of wild-type NES-H12, which was predominantly cytosolic (Fig. 8*C*). Similarly, both F401P+F401P and F401P+F401P,F405N showed a predominantly nuclear localization (Fig. 8*C*). These results further confirmed that mutants F401P and F401P,F405N are highly compromised in nuclear export. Taken together, these results provide evidence that Phe^{397}, Leu^{400}, and Phe^{401} are essential residues for the function of NES-H12 and suggest that secondary structure elements play an important role in the function of NES-H12. Finally, the type of amino acid replacement and the position of the change in the helical region are important factors that determine the relative strength of NES-H12.

Effect of NLS and NES Mutations on Transcriptional Activity—To gain further insight into the physiological significance of TR shuttling signals, we examined the transcriptional activity of GFP-tagged full-length TRα1, TRβ1, and select NLS and NES mutants. We predicted that disrupting the balance of nuclear import and export signals in TRα1 would have an effect on CAT reporter gene expression under control of a thyroid hormone-responsive element (TRE). To test our prediction, HeLa cells were transiently transfected with GFP-tagged TR expression plasmids, along with a TRE-CAT reporter plasmid, and analyzed by CAT ELISA (Fig. 8*D*). For the two TRα1 mutations tested that significantly disrupt NES-H12 (TRα1-F401A and TRα1-F401P), the levels of CAT protein produced in the presence of T_3 were reduced by 1.75-fold in TRα1-F401A and by 5-fold in TRα1-F401P. This finding highlights the complexity of teasing apart overlapping domains within this modular receptor. Both mutations reduce nuclear export and hence might be predicted to increase transcriptional output because of increased nuclear accumulation of TRα1. However, in fact, the mutation decreases transcriptional output, presumably because of interfering with the AF-2 transactivation function that also resides within helix 12.

In contrast, there was no change in transcriptional activation for TRα1 carrying the NLS-2 mutation, R26H, compared with wild-type TRα1 (Fig. 8*D*). This indicates that in the context of the whole protein a defective NLS-2 can be compensated by NLS-1; sufficient receptor is retained in the nucleus to activate T_3-mediated gene expression. Likewise, the absence of NLS-2 in native TRβ1 is compensated by NLS-1, and indeed, the receptor, at this particular palindromic TRE, is able to stimulate CAT reporter expression at high levels compared with TRα1 (Fig. 8*D*).

Mutations in NES-H12 Decrease the Rate of Shuttling of Full-length TRα1 and TRβ1—To further confirm that NES-H12 is necessary for efficient nuclear export of TRα1 and TRβ1, the inactivating mutation F401A was introduced in full-length TRα1, and the comparable F455A mutation was introduced in full-length TRβ1. Full-length TRα1 and TRβ1 are primarily localized to the nucleus at steady state; thus, to quantify changes in nucleocytoplasmic shuttling kinetics of GFP-tagged TR constructs, FRAP analysis was performed (Fig. 9). We predicted that these inactivating mutations in NES-H12 would result in a measurable decrease in the rate of TR shuttling between the cytoplasm and nucleus. Shuttling was visualized in real time by monitoring the exchange of GFP-tagged protein between two nuclei present in a single cell, after one nucleus was photobleached. The fluorescence recovery of the bleached nucleus was monitored over a period of 68 min. Average recovery rates from replicate experiments were plotted for control *versus* mutant TRs.

As predicted, the recovery rate for NES-H12 mutant TRα1-F401A was markedly slower in comparison with the control wild-type TRα1 (Fig. 9, *A* and *B*). At the end of imaging TRα1-F401A showed, on average, a 42.6% decrease in recovery rate in comparison with wild type, suggesting that export of the mutant from the unbleached nucleus was reduced, and hence, the amount of TR available for re-import into the bleached nucleus was decreased proportionally. Similarly, the recovery rate for NES-H12 mutant TRβ1-F445A also was markedly slower in comparison with the wild-type TRβ1 control. At the end of the imaging period, TRβ1-F455A showed, on average, a

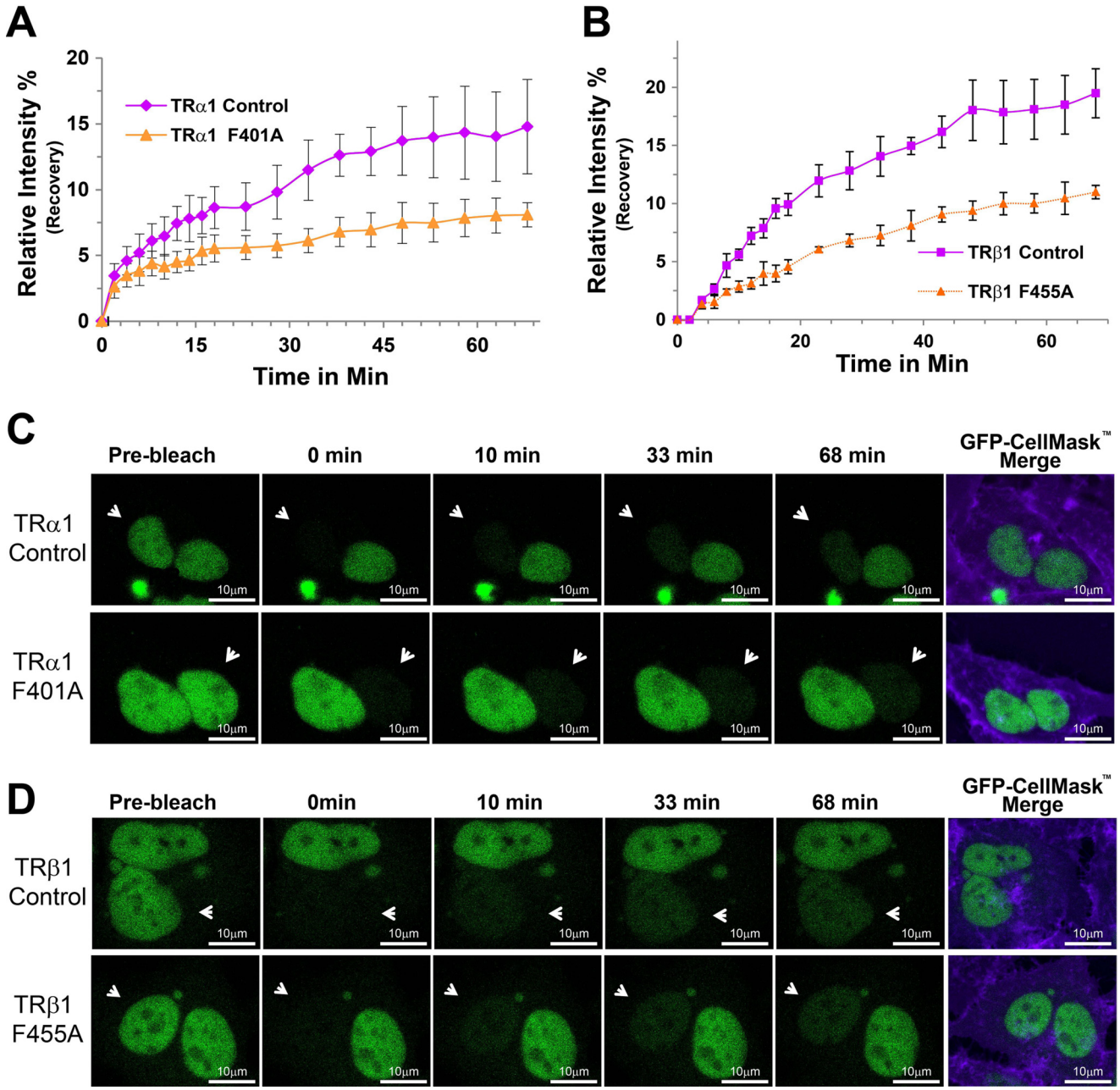

FIGURE 9. **TRα1 and TRβ1 NES-H12 mutants show reduced shuttling kinetics.** *A,* full-length GFP-TRα1 with the F401A mutation showed slower shuttling compared with wild type. The *graph* summarizes quantification of the rate of recovery of bleached nuclei in replicate FRAP experiments ($n = 4$). *Error bars* indicate ± S.D. *B,* full-length GFP-TRβ1 with the F455A mutation showed slower shuttling compared with wild type. The *graph* summarizes quantification of the rate of recovery of bleached nuclei in replicate FRAP experiments ($n = 3$). *Error bars* indicate ± S.D. *C* and *D,* representative FRAP images of recovery at different points from 0 to 68 min for TRα1 (*C*) and TRβ1 (*D*) WT and mutants, as indicated. *GFP-CellMask™ Merge*; merged images of GFP-tagged TR and CellMask™ deep red plasma membrane stain, confirming that two nuclei are present in a single cell. *White arrowheads* indicate bleached nuclei.

43.5% decrease in recovery rate in comparison with wild type (Fig. 9, *C* and *D*).

Taken together, these results confirm that NES-H12 functions as an active signal that is necessary for efficient nuclear export in the context of full-length TRα1 and TRβ1, and it is a transferable NES that can direct a heterologous nuclear protein to the cytosol.

DISCUSSION

Over the past several years there has been a dramatic shift in our view of TR subcellular distribution, from dogma of a primarily nuclear localization to recognition of the receptor's shuttling capability (6, 33). However, the precise mechanisms by which shuttling occurs and the specific NLS and NES motifs that cooperate in achieving this dynamic process previously were not fully understood. Here, we report on a detailed, comprehensive study of the specific molecular signal sequences involved in import and export. Our findings underscore the importance of domain architecture in regulating shuttling of TRα1. We show that two NLS sequences and multiple NES sequences, in combination, are involved in regulation of TRα1 shuttling (Fig. 10*A*), which in turn may

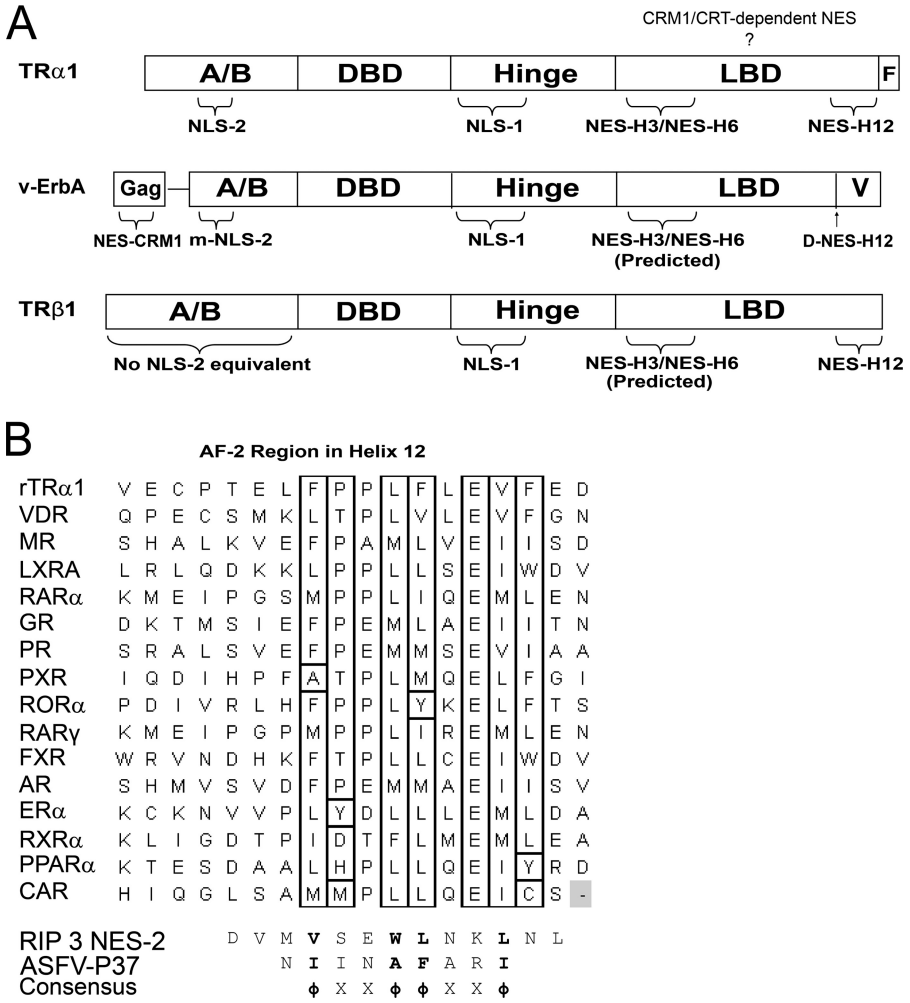

FIGURE 10. **TRα1 has multiple conserved signals for nuclear import and export.** *A,* schematic of location of NLS and NES motifs of TRα1, TRβ1, and v-ErbA. The positions of NLS, NES, and putative and predicted NES sequences are indicated in relation to the respective individual domains of TRα1. *NES-CRM1*, CRM1-dependent NES in the Gag region of v-ErbA; *m-NLS-1*, inactive NLS-1 equivalent in v-ErbA; *NES-H3/NES-H6 predicted*, based on the sequence identity with NES-H3/NES-H6 in TRα1; *V,* v-ErbA-specific C-terminal sequence; *D-NES-H12*, deletion of NES-H12 in v-ErbA. *B,* H12 regions from several members of the nuclear receptor family were aligned using ClustalW2 (69) and edited using CINEMA (46). Conserved hydrophobic residues are *boxed*. Individual amino acids showing significant changes are enclosed within a *square box*. Rat (*r*) TRα1; *VDR*, vitamin D receptor; *MR*, mineralocorticoid receptor; *LXRα*; liver X receptor α; *RARα*, retinoic acid receptor α; *GR,* glucocorticoid receptor; *PR*, progesterone receptor; *PXR*, pregnane X receptor; *RORα,* retinoic acid-related receptor α; *RARγ,* retinoic acid receptor γ; *FXR,* farnesoid X receptor; *AR,* androgen receptor; *ERα,* estrogen receptor α; *RXRα,* retinoid X receptor α; *PPARα,* peroxisome proliferator-activated receptor α; *CAR,* constitutive androstane receptor. The alignment of NES-H12 with the NES sequences from RIP3 and African swine fever virus (*ASFV-P37*) is also shown, followed by a proposed NES-H12 consensus sequence.

contribute to the regulation of expression of TR target genes.

The TRα1 helix 12/AF-2 transactivation region is highly conserved among nuclear receptors. Alignment of sequences of the AF-2 region among 16 members of the nuclear receptor family shows conserved hydrophobic amino acids in specific positions (Fig 10*B*). Based on these alignments, we propose that NES-H12 represents a novel class of CRM1-independent NES present in nuclear receptors. This finding acquires further significance because of the crucial role of AF-2 in ligand-dependent transcriptional regulation in TR and other nuclear receptors (27–29). Our findings point to the complexity of regulation involving the AF-2 region in TR; mutations that disrupt nuclear export also reduce transactivation of a T_3-dependent reporter gene. We propose that the H12/AF-2 region also serves as an NES among other members of the nuclear receptor family, in addition to its well characterized role in ligand binding and coactivator or corepressor binding. Finally, NES-H3 and NES-H6 are highly conserved in rat TRα1, human TRβ1, chicken TRα1, and v-ErbA (see Fig. 8*C*). Thus, we also propose that NES-H3 and NES-H6 in these TR variants function as NES motifs, in addition to their role in ligand binding and protein-protein interactions. Further experiments will be required to test this hypothesis.

Two NLS Sequences in TRα1 Regulate Nucleocytoplasmic Shuttling—We have identified a novel monopartite NLS in the A/B domain of TRα1 (NLS-2). Both the hinge domain NLS-1 and A/B domain NLS-2 are necessary for efficient nuclear localization of TRα1. For complete nuclear localization at steady state, however, the A/B domain, DBD, and hinge domain of TRα1 are all required. These findings suggest that many factors, in addition to NLS-1 and NLS-2, contribute to the nuclear import and retention of TRα1. For example, the N-terminal 13 amino acids are necessary for complete nuclear localization of

chicken TRα1 (47). In addition, auxiliary factors such as nuclear co-repressor (NCoR) and retinoid X receptor have been shown to promote enhanced nuclear retention of TRβ1 (12). Furthermore, our data show that the flanking sequences of the core basic amino acid residues may influence NLS-2 activity. The influence of nonbasic amino acids on NLS function has also been reported in earlier studies with nucleoplasmin and SV40 T-antigen (48). Strikingly, a change of Arg to His (equivalent of R26H in rat TRα1) results in inactivation of the NLS-2 region in the v-ErbA. Thus, inactivation of NLS-2 may be one of the factors mediating the predominantly cytosolic localization of v-ErbA at steady state and contributing toward its oncogenic properties and sequestration of TRα1 in the cytosol (10, 42).

There is more to the A/B domain, however, than a signal mediating nuclear import. An NLS-2-inactivating mutation in full-length rat TRα1 retains a substantial nuclear population, along with a cytosolic subpopulation. However, when the entire TRα1 A/B domain is deleted, the mutant has a completely cytosolic distribution. Thus, in addition to NLS activity, the A/B domain of TRα1 likely plays a role in other mechanisms that enhance nuclear retention. Along a similar line, the DBD was also essential for complete nuclear localization of TRα1. These data suggest that the A/B domain, DBD, and hinge region work in concert to maintain the predominantly nuclear localization of TRα1.

TRα1 and TRβ1 share significant sequence conservation, particularly in the hinge domain NLS-1 and the NES motifs characterized in this study. However, there are features that are distinct to each isoform, including the composition of the A/B domain. TRα1 has only 52 amino acid residues, whereas TRβ1 has 106 amino acid residues, and an NLS equivalent to TRα1 NLS-2 in the A/B domain is absent from TRβ1. We have shown that efficient TRα1 nuclear localization requires both NLS-1 and NLS-2. It is not clear at present how NES-H12 and NES-H3/NES-H6 in combination with NLS-1 contribute toward the nucleocytoplasmic shuttling of TRβ1. We and others have observed that TRβ1 has a small cytosolic population (12). Thus, this cytosolic subpopulation may reflect the altered balance of NLS and NES activity defined in this study. It is reasonable to speculate that TRβ1 may have other mechanisms, such as increased nuclear retention, to compensate for the lack of a second NLS in its A/B domain.

Comparison of TR from *Ciona,* which is proposed to be the ancestral receptor for TRα1 and TRβ1 (49), also showed no NLS equivalent to the TRα1 NLS-1. Even more curious is the fact that although TRα1 and TRβ1 have diverged in this region, TRα1 NLS-2 is highly conserved across the vertebrate species. In fishes (*Oryzias latipes* and *Danio rerio*) there is some divergence from other species. Nevertheless, the five basic amino acids KRKRK are fully conserved in this case as well. These five basic amino acids of TRα1 are part of transactivation function AF-1 (50, 51). Thus, NLS-2 may play a significant role in the overall function of TRα1, through its role both in nuclear import and in transactivation. NLS motifs in the A/B domain have been identified in other nuclear receptors as well. For example, LXRα and LXRβ, which are evolutionarily closely related to TRs, have a monopartite NLS at their N terminus, in addition to an NLS in their respective hinge regions (52). However, it is not clear if the NLS motif in these receptors also participates in transactivation function.

Multiple NES Sequences in TR Regulate Nucleocytoplasmic Shuttling—Previously, we identified a CRM1-dependent pathway for TRα1 nuclear export in which calreticulin plays a role as a chaperone (33). This CRM1-dependent NES remains to be identified. In addition, an earlier study suggested the presence of an NES in the TRβ1 DBD (41); however, in our current studies, the TRα1 DBD did not show NES activity capable of counteracting the NLS activities of either the hinge or A/B domains. Instead, our present study revealed the presence of three major regions with novel CRM1-independent NES activity in the LBD as follows: a C-terminal helix 12 region (NES-H12), the helix 3 region (NES-H3), and the helix 6 region (NES-H6). NES-H12, NES-H3, and NES-H6 all have transferable NES function, sufficient to target a nucleus-localized protein to the cytosol.

CRM1-dependent as well as CRM1-independent NES sequences have been identified among other nuclear receptors. For example, the constitutive androstane receptor has been shown to have both CRM1-dependent and CRM1-independent NES activity in the LBD (17, 18). Similarly, ERα contains a CRM1-dependent NES and a CRM1-independent NES (53), although AR appears to have only a CRM1-independent NES (54). Finally, the DBD of GR has been shown to have a CRM1-independent NES, and calreticulin plays a role in its export (41, 55–57), whereas peroxisome proliferator-activated receptor has NES motifs in the DBD and LBD that are recognized by calreticulin and CRM1, respectively (3). Thus, the presence of multiple NLS and NES motifs plays an important role in regulating the nucleocytoplasmic shuttling of nuclear receptors, including TRα1.

The distinct contribution of this study is the precise characterization of a short, novel, and transferable CRM1-independent NES. This characterization of a minimal NES sequence will facilitate rapid and reliable identification of similar CRM1-independent NES sequences among other nuclear receptors. Identification of such signals has been difficult not only because of a lack of information on a consensus sequence but also because of the complex nature of nuclear receptor shuttling. This complexity is illustrated by this study with various combinations of TRα1 domains, which indicate that transport signals alone may not be sufficient for the precise nuclear localization of TRα1.

It is clear that mutagenesis studies within the context of a whole protein need not necessarily correlate with the loss or gain of a specific NES or NLS. Altered intramolecular or intermolecular interactions that affect nuclear or cytoplasmic retention may also contribute to a change in the localization of a nuclear receptor. Thus, strategies were adopted in our studies to precisely and unambiguously separate the contribution of the transport signals from other contributing factors. This type of systematic functional characterization will also be useful in identifying interacting partners of nuclear receptors and the nature of their interactions.

Here, we have characterized the amino acid residues essential for NES-H12 function and propose a consensus sequence for this novel class of NES (Fig. 10*B*). Comparison of AF-2 sequences from a number of nuclear receptors reveals a high

degree of homology. Hence, the AF-2 region from other nuclear receptors may also have NES function. NES-H12 resembles the classical leucine-rich NES that uses a CRM1-dependent export pathway; however, it does not fit the consensus (2, 58). There are only a few examples of NES motifs that are leucine-rich but do not interact with CRM1. Examples include African swine fever virus protein p37 and human RIP3 protein (receptor interacting protein 3) (59, 60). Similar to NES-H12, these sequences have multiple hydrophobic residues. The consensus among the three is likely $\phi XX\phi\phi XX\phi$ (where ϕ is any hydrophobic residue, and X is any amino acid); however, more examples are required for higher reliability of prediction. Interestingly, NES-H12 is absent in v-ErbA; the major export activity of the oncoprotein is mediated by a strong CRM1-dependent NES present in the Gag region of this retroviral fusion protein (42).

In addition to precise characterization of NES-H12, we report the partial characterization of two NES motifs present in tandem in the H3/H6 region, NES-H3 and NES-H6. Based on our data showing that each motif functions separately as an independent transferable NES with two overlapping amino acid residues (see Fig. 6), we have classified them as two separate NES sequences rather than as a single bipartite NES. Similar to NES-H12, the NES-H3 and NES-H6 sequences also show conserved hydrophobic residues; however, a consensus sequence is not readily apparent among the three NES motifs.

The TRα1 H3/H6 and H12 regions form part of the ligand binding pocket (26). Because both of these regions have NES function, we propose that there is a relationship between ligand binding and nuclear export of TRα1. In support of this model, the aryl hydrocarbon receptor has two NES sequences; ligand binding influences the activity of both of the NES motifs, and depending on the ligand binding status, one or the other NES is active or inactive (61). Although it is known that TRα1 shuttling is not fully ligand-dependent (6), a detailed study of the effect of ligand binding on the kinetics of shuttling of TRα1 between the nucleus and cytoplasm has not been carried out. Such kinetic studies in live cells will be of importance for understanding the relationship between ligand binding and nucleocytoplasmic shuttling of TRα1 and TRβ1 and their effect on modulating the expression of TR target genes.

Nuclear Export and RTH—NES-H12 is 100% conserved between TRα1 and TRβ1, and this region is known as one of the hot spots of TRβ1 RTH mutations (26, 62, 63). One such mutation, L454S, shows increased corepressor binding and a 5-fold decrease in T_3 binding compared with the wild-type receptor (64). As a proof of principle, we showed that TRβ1 L454S (equivalent to TRα1 L400S) exhibits moderately reduced nuclear export. The reduced nuclear export activity of this mutant points to the intriguing possibility that defective nuclear export of TRβ1 may be a contributing factor to the pathology of RTH syndrome. Further studies are required to confirm and extend this hypothesis.

In addition to H12, the H3-H6 region also harbors two hot spots of RTH mutations (26, 65, 66). As we have demonstrated that two NES motifs of significant strength reside in this region, it seems likely that some of the RTH mutations in this region are compromised in nuclear export. Thus, despite the predominant nuclear localization of TRα1 and TRβ1, a precise balance in nucleocytoplasmic shuttling may be an important level of transcriptional regulation of TR target genes. Disruption of this precise balance may be one of the contributing factors toward the RTH phenotype. In view of these observations, in the future a systematic approach to therapeutics for RTH may need to take into account the possibility that altered nucleocytoplasmic shuttling of TR contributes toward hormone resistance.

Despite significant conservation of the DBD and LBD, TRα1 and TRβ1 show distinct differences in the shuttling, as evidenced by the difference in their nuclear transport signal composition revealed here. Characterizing such functional differences between the two isoforms has implications for the design of isoform-specific therapies. Along similar lines, the oncoprotein v-ErbA has significant alteration in its nuclear transport signal composition, through deletion, inactivating mutations, and addition of signals. Our comparative studies of these differences have provided significant understanding of the possible mechanisms underlying conversion of a normal nuclear receptor into an oncogenic variant (Fig. 10*A*) (9, 10, 42).

In summary, the presence of two NLS sequences and multiple NES sequences in TRα and their conservation among the vertebrate species suggest that nucleocytoplasmic shuttling is crucial for the normal function of TR. Altered nucleocytoplasmic shuttling due to defective nuclear export may be a contributing factor toward RTH syndrome and other nuclear receptor-related disorders. Importantly, NES-H12 likely represents a novel class of CRM1-independent NES sequences. Thus, this study serves as a critical starting point for characterizing similar NES motifs in other nuclear receptors and shuttling transcription factors that use exportins other than CRM1. Comprehensive analysis of the importins and exportins that bind each motif (3, 4, 67, 68) should help to clarify the mechanisms that regulate the multiple pathways followed by TR in its dynamic shuttling from the cytosol to nucleus. Finally, TR isoforms exhibit distinct differences in how shuttling is mediated, as evidenced by differences in their nuclear transport signal composition. Molecular characterization of isoform-specific differences in signals regulating the transport of TRα1 and TRβ1 may provide key insights for design of specific therapeutic molecules.

REFERENCES

1. McLane, L. M., and Corbett, A. H. (2009) Nuclear localization signals and human disease. *IUBMB Life* **61,** 697–706
2. Kutay, U., and Güttinger, S. (2005) Leucine-rich nuclear export signals. Born to be weak. *Trends Cell Biol.* **15,** 121–124
3. Umemoto, T., and Fujiki, Y. (2012) Ligand-dependent nucleo-cytoplasmic shuttling of peroxisome proliferator-activated receptors, PPARα and PPARγ. *Genes Cells* **17,** 576–596
4. Dopie, J., Skarp, K. P., Rajakylä, E. K., Tanhuanpää, K., and Vartiainen, M. K. (2012) Active maintenance of nuclear actin by importin 9 supports transcription. *Proc. Natl. Acad. Sci. U.S.A.* **109,** E544–E552
5. Vandevyver, S., Dejager, L., and Libert, C. (2012) On the trail of the glucocorticoid receptor. Into the nucleus and back. *Traffic* **13,** 364–374
6. Bunn, C. F., Neidig, J. A., Freidinger, K. E., Stankiewicz, T. A., Weaver, B. S., McGrew, J., and Allison, L. A. (2001) Nucleocytoplasmic shuttling of the thyroid hormone receptor α. *Mol. Endocrinol.* **15,** 512–533
7. Zhang, J., and Lazar, M. A. (2000) The mechanism of action of thyroid hormones. *Annu. Rev. Physiol.* **62,** 439–466
8. Lazar, M. A. (2003) Thyroid hormone action. A binding contract. *J. Clin. Invest.* **112,** 497–499
9. Bonamy, G. M., and Allison, L. A. (2006) Oncogenic conversion of the

thyroid hormone receptor by altered nuclear transport. *Nucl. Recept. Signal.* **4,** e008
10. Bonamy, G. M., Guiochon-Mantel, A., and Allison, L. A. (2005) Cancer promoted by the oncoprotein v-ErbA may be due to subcellular mislocalization of nuclear receptors. *Mol. Endocrinol.* **19,** 1213–1230
11. Laudet, V. (1997) Evolution of the nuclear receptor superfamily. Early diversification from an ancestral orphan receptor. *J. Mol. Endocrinol.* **19,** 207–226
12. Baumann, C. T., Maruvada, P., Hager, G. L., and Yen, P. M. (2001) Nuclear cytoplasmic shuttling by thyroid hormone receptors. *J. Biol. Chem.* **276,** 11237–11245
13. Casas, F., Busson, M., Grandemange, S., Seyer, P., Carazo, A., Pessemesse, L., Wrutniak-Cabello, C., and Cabello, G. (2006) Characterization of a novel thyroid hormone receptor α variant involved in the regulation of myoblast differentiation. *Mol. Endocrinol.* **20,** 749–763
14. Lee, Y., and Mahdavi, V. (1993) The D domain of the thyroid hormone receptor α1 specifies positive and negative transcriptional regulation functions. *J. Biol. Chem.* **268,** 2021–2028
15. Maruvada, P., Baumann, C. T., Hager, G. L., and Yen, P. M. (2003) Dynamic shuttling and intranuclear mobility of nuclear hormone receptors. *J. Biol. Chem.* **278,** 12425–12432
16. Zhu, X. G., Hanover, J. A., Hager, G. L., and Cheng, S. Y. (1998) Hormone-induced translocation of thyroid hormone receptors in living cells visualized using a receptor green fluorescent protein chimera. *J. Biol. Chem.* **273,** 27058–27063
17. Kanno, Y., Suzuki, M., Miyazaki, Y., Matsuzaki, M., Nakahama, T., Kurose, K., Sawada, J., and Inouye, Y. (2007) Difference in nucleocytoplasmic shuttling sequences of rat and human constitutive active/androstane receptor. *Biochim. Biophys. Acta* **1773,** 934–944
18. Kanno, Y., Suzuki, M., Nakahama, T., and Inouye, Y. (2005) Characterization of nuclear localization signals and cytoplasmic retention region in the nuclear receptor CAR. *Biochim. Biophys. Acta* **1745,** 215–222
19. Picard, D., and Yamamoto, K. R. (1987) Two signals mediate hormone-dependent nuclear localization of the glucocorticoid receptor. *EMBO J.* **6,** 3333–3340
20. Cadepond, F., Gasc, J. M., Delahaye, F., Jibard, N., Schweizer-Groyer, G., Segard-Maurel, I., Evans, R., and Baulieu, E. E. (1992) Hormonal regulation of the nuclear localization signals of the human glucocorticosteroid receptor. *Exp. Cell Res.* **201,** 99–108
21. LaCasse, E. C., Lochnan, H. A., Walker, P., and Lefebvre, Y. A. (1993) Identification of binding proteins for nuclear localization signals of the glucocorticoid and thyroid hormone receptors. *Endocrinology* **132,** 1017–1025
22. Kaku, N., Matsuda, K., Tsujimura, A., and Kawata, M. (2008) Characterization of nuclear import of the domain-specific androgen receptor in association with the importin α/β and Ran-guanosine 5′-triphosphate systems. *Endocrinology* **149,** 3960–3969
23. Cutress, M. L., Whitaker, H. C., Mills, I. G., Stewart, M., and Neal, D. E. (2008) Structural basis for the nuclear import of the human androgen receptor. *J. Cell Sci.* **121,** 957–968
24. Prüfer, K., and Barsony, J. (2002) Retinoid X receptor dominates the nuclear import and export of the unliganded vitamin D receptor. *Mol. Endocrinol.* **16,** 1738–1751
25. Kumar, R., and Thompson, E. B. (2003) Transactivation functions of the N-terminal domains of nuclear hormone receptors. Protein folding and coactivator interactions. *Mol. Endocrinol.* **17,** 1–10
26. Wagner, R. L., Apriletti, J. W., McGrath, M. E., West, B. L., Baxter, J. D., and Fletterick, R. J. (1995) A structural role for hormone in the thyroid hormone receptor. *Nature* **378,** 690–697
27. Baniahmad, A., Leng, X., Burris, T. P., Tsai, S. Y., Tsai, M. J., and O'Malley, B. W. (1995) The Tau 4 activation domain of the thyroid hormone receptor is required for release of a putative corepressor(s) necessary for transcriptional silencing. *Mol. Cell. Biol.* **15,** 76–86
28. Barettino, D., Vivanco Ruiz, M. M., and Stunnenberg, H. G. (1994) Characterization of the ligand-dependent transactivation domain of thyroid hormone receptor. *EMBO J.* **13,** 3039–3049
29. Danielian, P. S., White, R., Lees, J. A., and Parker, M. G. (1992) Identification of a conserved region required for hormone-dependent transcriptional activation by steroid hormone receptors. *EMBO J.* **11,** 1025–1033
30. Tomura, H., Lazar, J., Phyillaier, M., and Nikodem, V. M. (1995) The N-terminal region (A/B) of rat thyroid hormone receptors α1, β1, but not β2 contains a strong thyroid hormone-dependent transactivation function. *Proc. Natl. Acad. Sci. U.S.A.* **92,** 5600–5604
31. Wilkinson, J. R., and Towle, H. C. (1997) Identification and characterization of the AF-1 transactivation domain of thyroid hormone receptor β1. *J. Biol. Chem.* **272,** 23824–23832
32. Hollenberg, A. N., Monden, T., and Wondisford, F. E. (1995) Ligand-independent and -dependent functions of thyroid hormone receptor isoforms depend upon their distinct amino termini. *J. Biol. Chem.* **270,** 14274–14280
33. Grespin, M. E., Bonamy, G. M., Roggero, V. R., Cameron, N. G., Adam, L. E., Atchison, A. P., Fratto, V. M., and Allison, L. A. (2008) Thyroid hormone receptor α1 follows a cooperative CRM1/calreticulin-mediated nuclear export pathway. *J. Biol. Chem.* **283,** 25576–25588
34. Cook, A., Bono, F., Jinek, M., and Conti, E. (2007) Structural biology of nucleocytoplasmic transport. *Annu. Rev. Biochem.* **76,** 647–671
35. Pemberton, L. F., and Paschal, B. M. (2005) Mechanisms of receptor-mediated nuclear import and nuclear export. *Traffic* **6,** 187–198
36. Tran, E. J., Bolger, T. A., and Wente, S. R. (2007) SnapShot. Nuclear transport. *Cell* **131,** 420
37. Fried, H., and Kutay, U. (2003) Nucleocytoplasmic transport. Taking an inventory. *Cell. Mol. Life Sci.* **60,** 1659–1688
38. Robbins, J., Dilworth, S. M., Laskey, R. A., and Dingwall, C. (1991) Two interdependent basic domains in nucleoplasmin nuclear targeting sequence. Identification of a class of bipartite nuclear targeting sequence. *Cell* **64,** 615–623
39. Dang, C. V., and Lee, W. M. (1989) Nuclear and nucleolar targeting sequences of c-Erb-A, c-Myb, N-Myc, p53, HSP70, and HIV Tat proteins. *J. Biol. Chem.* **264,** 18019–18023
40. Nakai, K., and Horton, P. (1999) PSORT. A program for detecting sorting signals in proteins and predicting their subcellular localization. *Trends Biochem. Sci.* **24,** 34–36
41. Black, B. E., Holaska, J. M., Rastinejad, F., and Paschal, B. M. (2001) DNA-binding domains in diverse nuclear receptors function as nuclear export signals. *Curr. Biol.* **11,** 1749–1758
42. DeLong, L. J., Bonamy, G. M., Fink, E. N., and Allison, L. A. (2004) Nuclear export of the oncoprotein v-ErbA is mediated by acquisition of a viral nuclear export sequence. *J. Biol. Chem.* **279,** 15356–15367
43. Guermeur, Y., Geourjon, C., Gallinari, P., and Deléage, G. (1999) Improved performance in protein secondary structure prediction by inhomogeneous score combination. *Bioinformatics* **15,** 413–421
44. McGuffin, L. J., Bryson, K., and Jones, D. T. (2000) The PSIPRED protein structure prediction server. *Bioinformatics* **16,** 404–405
45. Dressel, U., and Baniahmad, A. (2001) in *Nuclear Receptors and Genetic Disease* (Burris, T. P., and McCabe, E. R., eds) pp. 59–96, Academic Press, San Diego
46. Parry-Smith, D. J., Payne, A. W., Michie, A. D., and Attwood, T. K. (1998) CINEM. A novel Colour INteractive Editor for Multiple Alignments. *Gene* **221,** GC57–GC63
47. Andersson, M. L., and Vennström, B. (1997) Chicken thyroid hormone receptor α requires the N-terminal amino acids for exclusive nuclear localization. *FEBS Lett.* **416,** 291–296
48. Makkerh, J. P., Dingwall, C., and Laskey, R. A. (1996) Comparative mutagenesis of nuclear localization signals reveals the importance of neutral and acidic amino acids. *Curr. Biol.* **6,** 1025–1027
49. Escriva, H., Manzon, L., Youson, J., and Laudet, V. (2002) Analysis of lamprey and hagfish genes reveals a complex history of gene duplications during early vertebrate evolution. *Mol. Biol. Evol.* **19,** 1440–1450
50. Hadzic, E., Desai-Yajnik, V., Helmer, E., Guo, S., Wu, S., Koudinova, N., Casanova, J., Raaka, B. M., and Samuels, H. H. (1995) A 10-amino acid sequence in the N-terminal A/B domain of thyroid hormone receptor α is essential for transcriptional activation and interaction with the general transcription factor TFIIB. *Mol. Cell. Biol.* **15,** 4507–4517
51. Hadzic, E., Habeos, I., Raaka, B. M., and Samuels, H. H. (1998) A novel multifunctional motif in the amino-terminal A/B domain of T3Rα modulates DNA binding and receptor dimerization. *J. Biol. Chem.* **273,**

10270–10278
52. Prüfer, K., and Boudreaux, J. (2007) Nuclear localization of liver X receptor α and β is differentially regulated. *J. Cell. Biochem.* **100,** 69–85
53. Lombardi, M., Castoria, G., Migliaccio, A., Barone, M. V., Di Stasio, R., Ciociola, A., Bottero, D., Yamaguchi, H., Appella, E., and Auricchio, F. (2008) Hormone-dependent nuclear export of estradiol receptor and DNA synthesis in breast cancer cells. *J. Cell Biol.* **182,** 327–340
54. Saporita, A. J., Zhang, Q., Navai, N., Dincer, Z., Hahn, J., Cai, X., and Wang, Z. (2003) Identification and characterization of a ligand-regulated nuclear export signal in androgen receptor. *J. Biol. Chem.* **278,** 41998–42005
55. Liu, J., and DeFranco, D. B. (2000) Protracted nuclear export of glucocorticoid receptor limits its turnover and does not require the exportin 1/CRM1-directed nuclear export pathway. *Mol. Endocrinol.* **14,** 40–51
56. Holaska, J. M., Black, B. E., Love, D. C., Hanover, J. A., Leszyk, J., and Paschal, B. M. (2001) Calreticulin is a receptor for nuclear export. *J. Cell Biol.* **152,** 127–140
57. Holaska, J. M., Black, B. E., Rastinejad, F., and Paschal, B. M. (2002) Ca^{2+}-dependent nuclear export mediated by calreticulin. *Mol. Cell. Biol.* **22,** 6286–6297
58. la Cour, T., Kiemer, L., Mølgaard, A., Gupta, R., Skriver, K., and Brunak, S. (2004) Analysis and prediction of leucine-rich nuclear export signals. *Protein Eng. Des. Sel.* **17,** 527–536
59. Eulálio, A., Nunes-Correia, I., Carvalho, A. L., Faro, C., Citovsky, V., Salas, J., Salas, M. L., Simões, S., and de Lima, M. C. (2006) Nuclear export of African Swine Fever virus p37 protein occurs through two distinct pathways and is mediated by three independent signals. *J. Virol.* **80,** 1393–1404
60. Feng, S., Ma, L., Yang, Y., and Wu, M. (2006) Truncated RIP3 (tRIP3) acts upstream of FADD to induce apoptosis in the human hepatocellular carcinoma cell line QGY-7703. *Biochem. Biophys. Res. Commun.* **347,** 558–565
61. Berg, P., and Pongratz, I. (2001) Differential usage of nuclear export sequences regulates intracellular localization of the dioxin (aryl hydrocarbon) receptor. *J. Biol. Chem.* **276,** 43231–43238
62. Ishii, S., Yamada, M., Satoh, T., Monden, T., Hashimoto, K., Shibusawa, N., Onigata, K., Morikawa, A., and Mori, M. (2004) Aberrant dynamics of histone deacetylation at the thyrotropin-releasing hormone gene in resistance to thyroid hormone. *Mol. Endocrinol.* **18,** 1708–1720
63. Umezawa, R., Yamada, M., Horiguchi, K., Ishii, S., Hashimoto, K., Okada, S., Satoh, T., and Mori, M. (2009) Aberrant histone modifications at the thyrotropin-releasing hormone gene in resistance to thyroid hormone. Analysis of F455S mutant thyroid hormone receptor. *Endocrinology* **150,** 3425–3432
64. Tagami, T., Gu, W. X., Peairs, P. T., West, B. L., and Jameson, J. L. (1998) A novel natural mutation in the thyroid hormone receptor defines a dual functional domain that exchanges nuclear receptor corepressors and coactivators. *Mol. Endocrinol.* **12,** 1888–1902
65. Takeda, K., Weiss, R. E., and Refetoff, S. (1992) Rapid localization of mutations in the thyroid hormone receptor-β gene by denaturing gradient gel electrophoresis in 18 families with thyroid hormone resistance. *J. Clin. Endocrinol. Metab.* **74,** 712–719
66. Collingwood, T. N., Wagner, R., Matthews, C. H., Clifton-Bligh, R. J., Gurnell, M., Rajanayagam, O., Agostini, M., Fletterick, R. J., Beck-Peccoz, P., Reinhardt, W., Binder, G., Ranke, M. B., Hermus, A., Hesch, R. D., Lazarus, J., Newrick, P., Parfitt, V., Raggatt, P., de Zegher, F., and Chatterjee, V. K. (1998) A role for helix 3 of the TRβ ligand-binding domain in coactivator recruitment identified by characterization of a third cluster of mutations in resistance to thyroid hormone. *EMBO J.* **17,** 4760–4770
67. Dzijak, R., Yildirim, S., Kahle, M., Novák, P., Hnilicová, J., Venit, T., and Hozák, P. (2012) Specific nuclear localizing sequence directs two myosin isoforms to the cell nucleus in calmodulin-sensitive manner. *PLoS One* **7,** e30529
68. Fukumoto, M., Sekimoto, T., and Yoneda, Y. (2011) Proteomic analysis of importin α-interacting proteins in adult mouse brain. *Cell Struct. Funct.* **36,** 57–67
69. Larkin, M. A., Blackshields, G., Brown, N. P., Chenna, R., McGettigan, P. A., McWilliam, H., Valentin, F., Wallace, I. M., Wilm, A., Lopez, R., Thompson, J. D., Gibson, T. J., and Higgins, D. G. (2007) Clustal W and Clustal X, version 2.0. *Bioinformatics* **23,** 2947–2948